A PMMA CONDUCTIVITY PRETREATMENT MICROFLUIDICS DEVICE FOR THE OPTIMIZATION OF ELECTROKINETIC MANIPULATIONS

A Thesis

presented to

the Faculty of California Polytechnic State University,

San Luis Obispo

In Partial Fulfillment

of the Requirements for the Degree

Master of Science in Biomedical Engineering

by

Cameron Paul Purcell

June 2011

© 2011

Cameron Paul Purcell

ALL RIGHTS RESERVED

COMMITTEE MEMBERSHIP

TITLE: A PMMA CONDUCTIVITY PRETREATMENT MICROFLUIDICS DEVICE FOR THE OPTIMIZATION OF ELECTROKINETIC MANIPULATIONS

AUTHOR: Cameron Paul Purcell

DATE SUBMITTED: June 2011

COMMITTEE CHAIR: David Clague, Ph.D.
Associate Professor, Biomedical and General Engineering
California Polytechnic State University, San Luis Obispo

COMMITTEE MEMBER: Dan Walsh, Ph.D.
Professor, Materials Engineering
California Polytechnic State University, San Luis Obispo

COMMITTEE MEMBER: Robert Crockett, Ph.D.
Director, General Engineering Program
California Polytechnic State University, San Luis Obispo

ABSTRACT

A PMMA CONDUCTIVITY PRETREATMENT MICROFLUIDICS DEVICE FOR THE OPTIMIZATION OF ELECTROKINETIC MANIPULATIONS

Cameron Paul Purcell

This project encompasses the design and development of a pretreatment microfluidic device for samples of physiological conductivity, namely a saline solution. The conductivity was reduced through the combination of dilution and ion removal using electric fields to enable downstream electro kinetic manipulations. The two major parts of this project include (1) designing a pretreatment protocol to reduce the conductivity of the sample solution to an acceptable level and (2) designing /fabricating a microchip that will effectively allow aim (1) to be performed on chip.

This project is one of the first to observe the effects of an electric field, used in the application of ion removal, to reduce the conductivity of a sample. Through the combination of sample and low conductivity buffer, as well as the presence of an electric field, a conductivity pretreatment chip is created. Since biomarkers and analytes of interest are difficult to detect in complex raw samples, such as blood, this chip is a necessary preliminary step that allows for successive separations.

Using previous literature from the field of capillary electrophoresis, a design and pretreatment protocol was developed to pretreat a sample into a target conductivity range. A PMMA device was fabricated using a laser photoablation system located on the Cal Poly campus. Off-chip electrodes were used to induce electrophoretic movement of ions across a membrane and out of the sample. The combination of dilution and electrical fields yielded samples that had their conductivity reduced 80%. Dilution was found to be more effective in a chip designed with a short process time and continuous flow. Ultimately, we wish to incorporate this device with other pre-fabricated pretreatment and electrokinetic devices to optimize certain bioseparations.

Keywords: Pretreatment, Microfluidic, Laser, Conductivity, Ion, PMMA

ACKNOWLEDGMENTS

I would first like to thank Dr. David Clague for his direction, which was always given with a smile. His enthusiasm for his students and research helped provide momentum for this thesis.

Additionally, I would like to thank my committee members, Dr. Walsh and Dr. Crockett, for their assistance in the writing and defense process and for all their encouragement throughout this project.

I'd like to thank all the members of the Cal Poly Biofluidics group for all of their help and support throughout this project. Without your presence in the lab on those long nights, this thesis may never have seen its conclusion. Special thanks go out to Tim Abrams and Evan Barbre for paving much of the way for this project to happen and for continued support despite their graduation.

Finally I'd like to thank my family for their endless love and support throughout my entire academic career and for being a constant source of motivation.

TABLE OF CONTENTS

LIST OF TABLES

LIST OF FIGURES

I Introduction/Background

1.1 Point of Care Diagnostics

For over a decade Lab-on-a-chip (LOC) technologies, which are hand held devices that are designed to perform miniature laboratory analyses, have tantalized medical researchers as a solution to global health issues. Since global health is becoming an increasing concern for the international community as borders begin to dissolve and awareness of the cost benefits of preventative care increases, the need in developing countries for a low cost and effective means to diagnose illness on site has become paramount. This need is often referred to as point of care (POC) diagnostics, as it intends to provide healthcare outside of laboratories and medical facilities and instead bring it to the schools, homes and workplaces of the world. POC requires a diagnostic solution that is portable and inexpensive, as well as the capability to be operated by someone with no medical or technical training. These requirements must be met as its greatest application will be in countries without comprehensive healthcare systems [1]. While LOC technologies promise in principle to meet these requirements, they have yet to reach this goal due to several major obstacles yet to be overcome. One major hurdle is overcoming the difficulties presented by trying to handle raw samples, which are in no condition to be analyzed.

The first diagnostic tests were originally performed at the bedside and, hence, the point of care; however, as more sophisticated tests were developed, the tests began to be moved to a centralized laboratory. Today, lab tests play a key role in 60 to 70 percent of all diagnostic decisions [2]. However, a POC diagnosis is motivated by more than just the convenience of being able to provide medicine anywhere; it is also motivated by a need to provide quick and accurate

information in environments where a traditional laboratory is not available. While traditional Laboratories are capable of providing accurate results, they often take large amounts of time, are limited by technical staff and equipment, and are not easily accessible to most of the world. POC diagnostics do not require the transport of samples or persons to such facilities, which can be costly and difficult due to their sensitive nature, and can be performed in just about any situation. For example, during natural disasters where traditional medical facilities are overstretched or inaccessible, these devices could provide critical knowledge allowing proper, quick, and effective treatment. Additionally, POC diagnostics can provide illness screenings that will protect hospital patients from exposure to contagious diseases by keeping those cases from entering the hospital, provide the potential for higher and faster turnover rates, and improve many prognoses due to early detection [1]. While our research group is not solely designing devices that are to operate in poorer developing countries, the design constraints that these environments provide were strongly considered throughout the design process. In particular, our group has focused on creating devices that can be manufactured simply and as cost effectively as possible.

1.2 Elemental design of POC devices

As the ultimate goal of a LOC has yet to be realized, the general approach to achieving the goal of a deployable assay is to compartmentalize the system into functional sub elements with discrete functions. Thus, the design, fabrication, integration, and packaging problems for this concept are broken down into components that are manageable, feasible, and specific. Hence, instead of trying to design a chip that performs all essential system functions such as sample collection, pretreatment, analysis, and diagnosis, microfluidic chips have generally worked in one of these specific areas with the idea that future designs will be able to interconnect these components into one cohesive whole. With this approach, the general

function of a full scale laboratory can be miniaturized effectively into a lab instrument component. A chip designer can take a particular element of the laboratory, like a centrifuge, and work to miniaturize that individual apparatus into a set of microfluidic chips. Thus, as each piece of equipment in a laboratory is recreated on a chip and integrated together, you eventually achieve a lab on a chip. This approach makes use of the trend in industry to continue to miniaturize their products and therefore the amount of sample required for proper operation [3]. This also allows for successful chips to be implemented and put into use in laboratories prior to completion of the overall LOC design.

Breaking down this challenge into different areas of function is a paradigm that the Cal Poly Biofluidics Group has adopted. This paradigm, seen in figure 1, provides emphasis on the big picture of LOC technologies while illustrating the other devices and functions with whom a particular chip will interface.

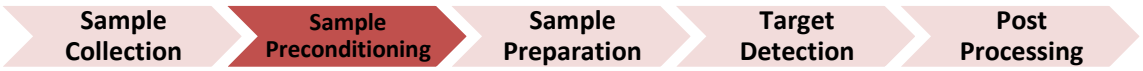

Figure 1: Lab on a chip functional area paradigm

The paradigm aids by compartmentalizing the system and by additionally illustrating the need for interconnection between system functions, a major obstacle that still needs to be overcome in this field. This project falls under the sample pretreatment regime and thus

works with the products of sample collection and provides a sample-to-sample concentration or separation.

1.2.1 Sample Collection

Sample Collection, the first step in any medical analysis, is one of the most important aspects of the process, as it determines the success and accuracy of everything that follows [4]. It is critical to take a sample that is representative of the population which is to be tested. Extra care must be taken with microfluidics chips to ensure that the small volume of sample that is processed by the chip is actually the intended sample. The most common errors from sampling are from contaminating the sample and from using the wrong sampling technique [4].

When developing a chip aimed at sample pretreatment, one must consider the samples that will be collected for POC applications. POC applications of LOC technologies will use biological fluids to conduct tests. This will mostly consist of bodily fluids such as blood, urine, sweat or saliva.[4] If these fluids were introduced into a microfluidic device in their raw form, there is a large potential to cause issues with the device as many of these fluids have formed elements within them that are capable of fouling a chip by clogging channels, filters, or pumps.

Since the aim of this project is a proof of concept for this approach to reduce conductivity, we used samples that are a simple combination of reagent grade salt and water. The ionic concentrations of the solutions were tailored to mimic those of bodily fluids such as blood, urine and sweat. Those ionic concentrations found in literature and used as guidelines to create our solutions are shown in table 1 below.

Table 1: Human biological fluids conductance from literature

Human Biological Fluid	Conductivity (mS/m)
Blood	667[5]
Plasma	1,443[6]
Urine	1,870[7]
Cerebral Spinal Fluid	1,457 [8]

We believe this is a reasonable approach, as this chip for conductivity conditioning is intended to be used with human biological samples. While these solutions do not include proteins and other larger molecules or formed elements, one of primary foci of this initial project is to prove that overcharged electrodes can create an electric field sufficient to remove ions from a solution and thereby lower that solution's conductivity.

1.2.2 Sample Pretreatment

The aim of sample pretreatment or sample conditioning is to manipulate a sample such that it can be easily handled by the downstream processes. Unfortunately, most raw samples are in a state that is not conducive to treatments used to extract information from a sample. Over 80 percent of analysis time is spent on the sampling and sample pretreatment steps [9]. In a previous work by

the Cal Poly Biofluidics Group [10], several key parameters were outlined as being necessary to pretreatment in order to provide a sample that will be useable by sample preparation or target detection chips downstream. These parameters included fluid viscosity, pH, and electrical conductivity. In Abrams' work, bovine calf serum was successful treated for fluid viscosity and pH. However, it was difficult to pretreat for electrical conductivity with the previous chip design, which will be discussed in further detail later. In this project, we use a different chip design and approach to treat a sample for electrical conductivity. Electrical conductivity is particularly important for target detection chips that make use of electrokinetics, or a method of using electrical phenomenon to manipulate particles, as it is the primary mechanism by which they work. Additionally, these chips are susceptible to electrolysis and Joule heating[11]. Therefore, this pretreatment chip is an essential step for downstream chips that depend on these electro kinetic manipulations.

1.2.3 Sample preparation

While sample preparation is similar to sample pretreatment in some regards, its focus is more on separating and concentrating a particular analyte. Often when performing analysis of a sample there is a given target, or analyte, that is of interest amongst a background of other proteins, ions, etc. These background molecules serve to create noise in the analysis and weaken the test's ability to create accurate results pertaining to the analyte of interest. For this reason, it is necessary to increase the concentration of the target compared to the background. Since more of the target cannot simply be created, it is necessary to remove as much of the noise as possible, thus relatively increasing the concentration. Methods to purify the system have become increasingly important as a growing area of interest in microfluidics is electrokinetic chips that perform separations of fluid samples. These electrokinetic chips make use of molecules' unique

electrophoretic mobility to separate them from each other. Eletrophoretic mobility refers to the ability of an analyte to move relative to the fluid in which it is suspended when it is subjected to an electric field. Since the one of the two contributing factors, size and charge, to an analyte's mobility is affected by conductivity, pretreatment of electrical conductivity is essential to successful operation of these electrokinetic chips. Without such preparation, targets can be difficult to detect or fall outside of detection limits entirely.

1.2.4 Detection/ Post processing

At the end of these other steps lies a final process to determine if a target will be discovered, found missing, or left undiscovered. A traditional approach from immunology research is often applied to microfluidics to this aim. This process involves the use of antigens in combination with a detectable physical change to determine if a target is in a sample. More specifically, molecule-specific antibodies that will exclusively bind with the target are connected with other molecules such that when they bind, detectable changes occur. These changes include a release or drop of heat, a change in optical properties that will cause the bound pair to absorb, reflect or diffract light, or a change in electrical conductivity. These measured changes are converted to an electrical signal that software can translate into an appreciable result of type and/or quantity. However, in spite of sample preparation and concentration, there is usually a significant amount of noise remaining in the measurement that requires post processing. Post processing can be an essential step to put the data into a format suitable for analysis by a user.

1.3 Pretreatment Introduction

1.3.1 Why pretreatment is necessary

For the aims of this particular project, we will continue to refer to its goal as sample pretreatment although the term applies to a wide variety of manipulations. Generally speaking, sample pretreatment is the step that lies between sample collection and sample preparation and involves the majority of the sample conditioning that optimizes the sample for the following steps. Sample pretreatment is a broad term since it can include a number of applications such as centrifugation, dilutions or condensing, enzymatic breakdown of substrates, mixing, use of buffers, heating and cooling, and deionization, in the case of this project. There are numerous other applications unlisted, but pretreatment encompasses anything that prepares a sample for its application in the downstream device.

Prior to microfluidics, these processes where performed in full-scale bench top equipment found in laboratories. The processes often involved huge samples by comparison that were often added to during the pretreatment process. As well, the equipment used to perform sample pretreatment required a trained or skilled worker to handle and process the sample. Some sample pretreatment processes involve the use of many different pieces of equipment and thus also involve significant sample handling. Since the designated purpose of POC diagnostics is to bring analysis to the site where the sample was gathered, this traditional approach to sample pretreatment is not a valid option. Furthermore, this analysis has the potential to be performed in just about any environment, even extreme ones, therefore, it follows that sample pretreatment should occur within the same device that will perform the analysis.

Processing the sample outside of the device, or off-chip, raises several concerns. One major concern is that this will require more handling of the sample which is dangerous for several reasons. The first is that in a POC environment, the handler of the sample may not be properly trained to perform such tasks. Ensuring that a sample remains uncontaminated and does not pose

a toxic biological risk requires training and skills that a common individual will not possess. Additionally, this handler will have to interact with the sample pretreatment device appropriately to get an accurate and correct result. The technical knowhow can vary substantially depending upon the device, but having the pretreatment off-chip will definitely require more steps than on-chip. The other major concern is that a traditional approach to pretreatment will require a bench top scale device that is not portable and would limit where this analysis could be performed.

To combat these concerns, the Cal Poly Biofluidics Group has proposed to design and develop an on-chip microfluidic pretreatment chip. This chip will be integrated with other chips to create a singular system capable of doing an entire laboratory instrument function on-chip, from sample collection to sample analysis. To ensure the feasibility of this directive, several considerations have been made. The chip will be designed and fabricated using previously established micro-fabrication techniques. Additionally, the chip will be designed to be low cost and error on the side of simplicity to ensure that the component can be integrated into a full system easily and applicably as a POC device. However, since experimentation will be required on this component to ensure it functions properly, it will be built as a functional independent component without any other preceding or succeeding chips.

1.3.2 Current Pretreatment Strategies

Unfortunately, there is no sample pretreatment procedure that works for all biological samples because there is such a large variety of potential samples and target analytes. While on-chip pretreatment has made significant progress in some areas such as adding buffers, mixing, and aliquoting, pretreatment of variable raw samples has yet to be performed[3]. Generally, the pretreatment performed on the sample is specifically chosen based upon the target analyte and the sample that is containing it. In a traditional laboratory, the methods for pretreatment almost

always result in an aqueous solution even if the raw sample is not. This can involve processes like solubilization, decomposition, dissolution and extraction [12]. While this is promising with regards to microfluidics as a whole, the processes listed that allow movement from more solid samples to liquid are not easily accomplished on a microfluidics chip. Additionally, pretreatment in the lab also involves the more commonly known processes of filtration, distillation, amplification, dilution, and centrifugation [13]. With such a wide array of processes falling within the domain of pretreatment, it is not surprising that an all-encompassing solution does not yet exist for pretreatment on chip. It then follows that there is a wide variety of bench top pieces of equipment in a traditional laboratory that perform sample pretreatments depending upon the procedure and that often, even in modern laboratories, the equipment currently used for pretreatment is not sophisticated enough to take a raw sample all the way through analysis without multiple steps and pieces of equipment [14].

Thus, there isn't one solution to all pretreatment needs that could be designed into a microfluidics chip. However, there are trends that provide an opportunity for pretreatment microfluidics to condition a sample successfully for certain downstream processes. For example, most pretreatment processes involve concentrating or isolating the analyte of interest from the background, such as removing albumin from other proteins of interest or separating key DNA fragments from their strands. Many microfluidic devices have successfully demonstrated such separations with a narrow focus [15]. As well, all pretreatment protocols serve to deliver a product that is agreeable with the technique that will be used to detect or analyze the analyte of interest.

Unfortunately, as Verpoorte et al. states, the number of microchips that have actually been employed to analyze physiological samples is few. Most literature reviews of sample

pretreatment on chip focus on separations and the tail-end of the lab-on-a-chip paradigm. In other words, most publications do not discuss the methods used to pretreat raw samples nor the initial stages of sample preparation. For this reason, the Cal Poly Biofluidics Group has sought to focus on pretreatment of raw samples with the aim of optimizing them for further manipulation downstream.

1.3.3 Goals for Project

Pretreatment of raw samples is an often-ignored area of the lab-on-a-chip paradigm. Most microfluidic chips are designed for detection and separation and most use preconditioned samples to accomplish their goals. This project, in addition to others in our group, aims to develop awareness of the importance of addressing issues with raw samples. We believe this to be of such importance because POC diagnostics will require working with raw samples.

The most popular type of microfluidic chips are those that are electrokinetically driven[15]. The Cal Poly Biofluidics Group has several projects that directly use electrokinetic manipulations to perform separations and analysis, such as dielectrophoresis (EEP), isotachophoresis (ITP), isoelectric focusing (IEF), and free flow electrophoresis (FFE). Thus, the product of this project has been chosen to provide these other projects with a means to have their samples conditioned on chip, prior to their own use of the sample. When this chip is integrated and combined with these other chips in the future, it is our hope that a raw sample could be introduced, processed, and analyzed all on chip thus creating a lab on a chip.

Most electrokinetic manipulations that would follow a pretreatment step require a reduction of the sample's electrical conductivity. This allows the manipulations to have considerably

more resolution due to the influence of electrical conductivity on electroosmotic flow and a particles' electrophoretic mobility, two principles that will be discussed in more detail later. Two other key properties, pH and viscosity, affecting electrokinetic manipulations were addressed by the precursor project. Therefore the pretreatment regimen proposed for this device was designed to lower the conductivity of a raw sample.

The goals of this project include: 1) demonstrating knowledge of current pretreatment techniques; 2) scaling down a bench scale conductivity pretreatment protocol into a microfluidic device; 3) designing, manufacturing, and testing a microfluidic chip; 4) verifying conductivity reduction on chip by experimentally observing the chip's influence on the sample; 5) reducing the conductivity of the sample by an order of magnitude; and 6) producing these effects rapidly on chip within five minutes. Our project will be deemed successful if these goals are met.

1.4 Electrophoresis Background

1.4.1 History and Background of Electrophoresis

Electrophoresis has been a standard tool for the analytical chemist or biologist since Arne Tiselius' experiments on moving boundary set the foundation for electrophoresis during the 1930's [16]. The term electrophoresis describes the motion of charged particles in solution when they are subjected to an electric field. Early Electrophoresis was not without its problems and limitations, however, due to its incomplete separation of proteins and the large volume of sample required. Over the next several decades, improvements were made and in the late 1960's polyacrylamide gel electrophoresis (PAGE) was developed to be used in

conjunction with sodium dodecyl sulfate (SDS). SDS-PAGE, or gel electrophoresis as it is commonly known, is a rapid and inexpensive method for characterizing protein mixtures and determining protein monomer molecular weights [16]. For this reason, gel electrophoresis has been and continues to be one of the most used protein analysis methods in analytical chemistry for more than twenty years [17].

During most electrophoretic processes, including this one, proteins are separated by their net charge and their size. Very simply, the gel acts to constrict movement of proteins based upon their size.The SDS is a detergent or surfactant that, when added to the sample, works to encapsulate the proteins and makes them all appear to have the same negative charge [18]. The sample containing the proteins is loaded into the gel at the 'top' and a voltage is applied from this region toward the direction of flow. The draw of the electric field and the resistance of the gel act to stratify the proteins into discrete regions by those parameter's effects on them. This results in the image seen below (figure 2), where the proteins can clearly be seen separated from one another by their size, or number of base pairs, and their charge.

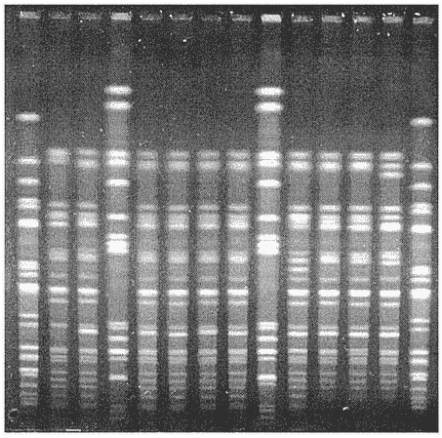

Figure 2: Gel electrophoresis example. Each of the vertical lanes represents a solution that was tested and each of the horizontal stripes represents a protein fraction [19]

However, in SDS-PAGE the reliance on size as the separating mechanism makes effectively separating smaller, lower weight molecules difficult. And many of the biomarkers of interest, especially recently, are small, low weight, biomolecules that gel electrophoresis essentially can't handle [20].

Two classes of species that are of particular interest to this project are proteins and ions, both of which can be manipulated by electrophoresis. However, as mentioned before, ions are much, much smaller than proteins. As a result, gel electrophoresis is not a good technique for working with ions. This led to the development of a related technique called capillary electrophoresis.

1.4.2 Capillary Electrophoresis

Another eletrophoretic technique that is less common but arguably more effective is capillary electrophoresis. Capillary electrophoresis creates a current through a capillary tube by placing electrodes at both ends of the very narrow tube. The electric field created in the tube works to accelerate or decelerate charged species in the tube [16]. Capillary electrophoresis is advantageous over gel in that traditional gel electrophoresis does not disperse heat well and thus must be run at lower voltages (40 V/cm versus up to 800 V/cm for gel capillary electrophoresis [16]) causing longer experiment times. Additionally, the gel is time consuming to prepare in comparison and requires more sample to process a experiment. However, more importantly, capillary electrophoresis handles ionic species and smaller molecules better by being more dependent on the species charge.

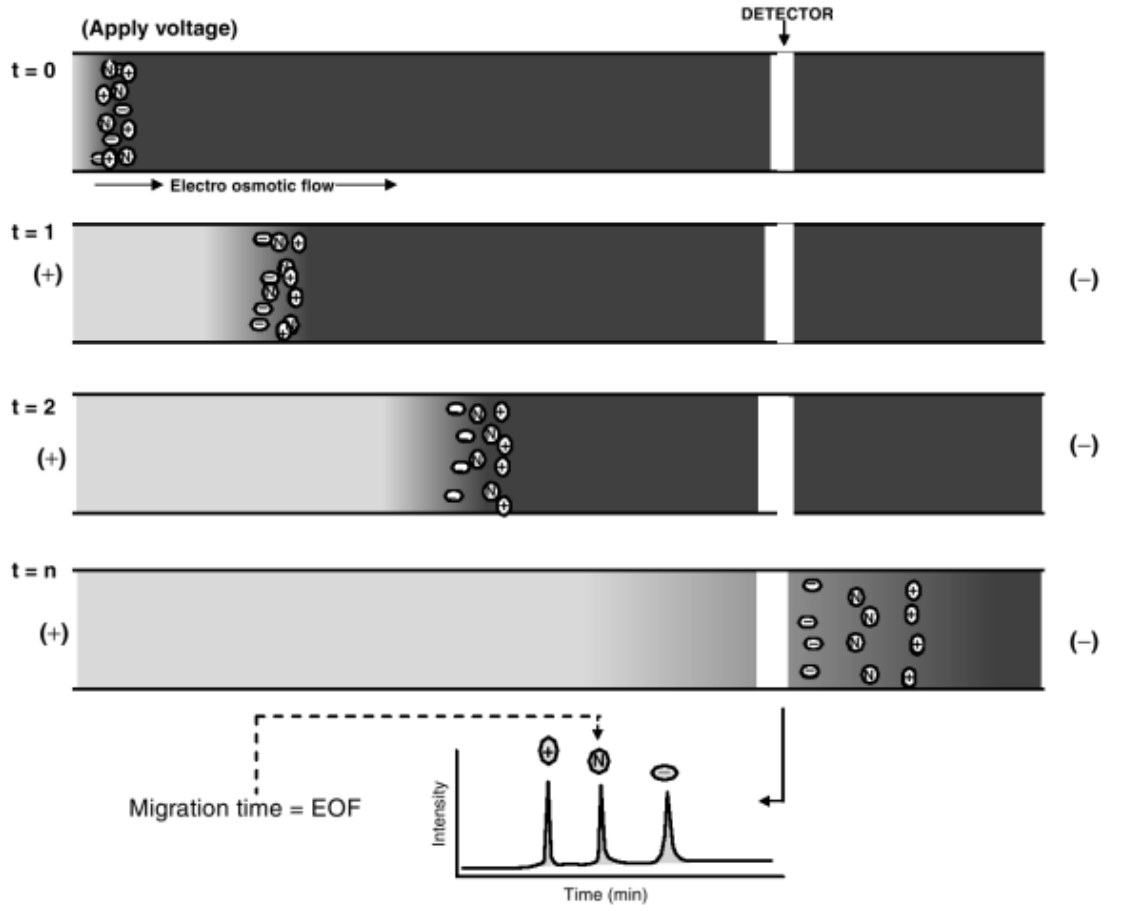

Figure 3: Mobility of charged and uncharged molecules in an applied field [21]

The movement of a species in a capillary tube is controlled primarily by two forces. The first is the electrophoretic force which is a result of the electric field pushing or pulling a charged particle. The other is the electroosmotic force which is a result of the fact that silica (as well as PMMA) imparts a negative charge on the inner surface of the capillary tube. This results in a net movement of fluid toward the cathode. This phenomenon results in all species moving toward the cathode and can be seen as the negative terminal in Figure 3. These two phenomena in conjunction cause the species to form into unique stacks or zones that can be detected as they exit the capillary tube. The species of greatest net charge will be found in the

leading and following zones, while those that are more electrically neutral will be found between them. Performing electrophoresis in a tube has the added benefit that the tube can be used multiple times. Due to the scale and nature of microfluidic chips, any electrokinetics performed on chip behave very similar to those of capillary electrophoresis. For a more detailed treatment of electrophoresis theory please refer to Appendix A.

1.4.3 Buffer / pH influence on above and future separations

As previously mentioned, changes in pH conductivity strongly influence electrokinetic manipulations. This is a result of the parameters having an influence on both electroosmotic and electrophoretic flow. The solution's pH influences the amount of surface ionization of the stationary phase, which will in turn change its potential, the zeta potential. A high pH will produce an increase in [EO] flow; a low pH will have an inverse effect. In addition, pH affects the amount of ionization of the particles themselves. This ionization, in turn, affects the particles' electrophoretic mobility by increasing or decreasing its ionic charge.

When the conductivity, or ionic strength, of the solution increases, the electroosmotic flow will decrease due to a lower zeta potential. Just as with pH, conductivity also affects the surface charge of particles and thus their electrophoretic mobility. In both cases, an increased conductivity results in a larger screening length, which essentially shields the particle and stationary phase from the electric field.

Understanding the impact of the pH and conductivity on electrokinetics is important to this project, for it is these properties that motivate it. A properly chosen solution with a balanced pH will therefore be an important aspect. Additionally, the conductivity of the sample

solution will need to be high enough to demonstrate the effectiveness of the chip, but not so high that it disturbs functionality by negatively impacting the electrokinetic flow.

1.4.4 Media Background Used in This Thesis

While it would be ideal to use a solution that demonstrates this chip's ability to remove ions from a sample without disturbing other analytes, we chose to focus on one of the main goals of this project, the demonstration that removing ions with an electric field is feasible on chip. If ions can be removed using this method, then the conductivity will also be lowered and the end goal of this project will be achieved. We are confident that filtration techniques and materials that are capable of preventing larger molecules from passing without preventing the passage of ions exist. As well, other methods exist that do not involve filters. Should a filter system not be successful, we believe that other approaches, like liquid-liquid extraction, could incorporate this approach. Thus, we have chosen to use a more simple solution that contains only water and reagent grade salt so as not to complicate the data with other analytes. The water acts as the solvent and the reagent grade salt acts as the solute and the source of ions.

1.5 Laser Processing

For this project, the chosen manufacturing method for making the microfluidic chip was to use a laser engraving machine. Lasers, which stand for "light amplification by stimulated emission radiation," have been around for decades and can be found in a wide variety of applications, including manufacturing medicines and even simple light shows.

1.5.1 Laser Power

Laser power is usually defined in units of watts or watts per area. The laser used in this project was 120 watts and was a part of the Universal Laser Systems X2-660. The machine is located in the Bonderson building within the Mustang 60 Machine Shop on the Cal Poly campus. The laser cell used by this machine is essentially a plasma tube filled with carbon dioxide and other gases. The radio frequency electronics create a 40MHz standing wave within the plasma tube, thereby converting electrical energy into light energy [22]. According to the laser's operations manual, it emits photons at a frequency of 10.6 microns, and has a beam diameter of .005 inches. The laser system features settings that allow one to control its power, speed, and pulse density, or pulses per inch (PPI). PPI is a consequence of the system not being continually on; in other words, the laser turns on and off very quickly, creating pulses. This laser has a maximum resolution of 1000 PPI, which means the distance between pulses is around 25 microns. This setting was used for all cuts due to the detailed nature of microfluidic chip design.

The laser is generally configured to either etch the material or cut through the material. Power settings for through cuts are much higher than those for etching. For example, through cuts used a power setting of 45 (out of 100) and a speed setting of 2 (out of 100), while engraving used a power setting of 5 and speed setting of 7. Unfortunately, the laser does not have an even power distribution throughout the beam. In fact, the power density is more similar to a Gaussian distribution.

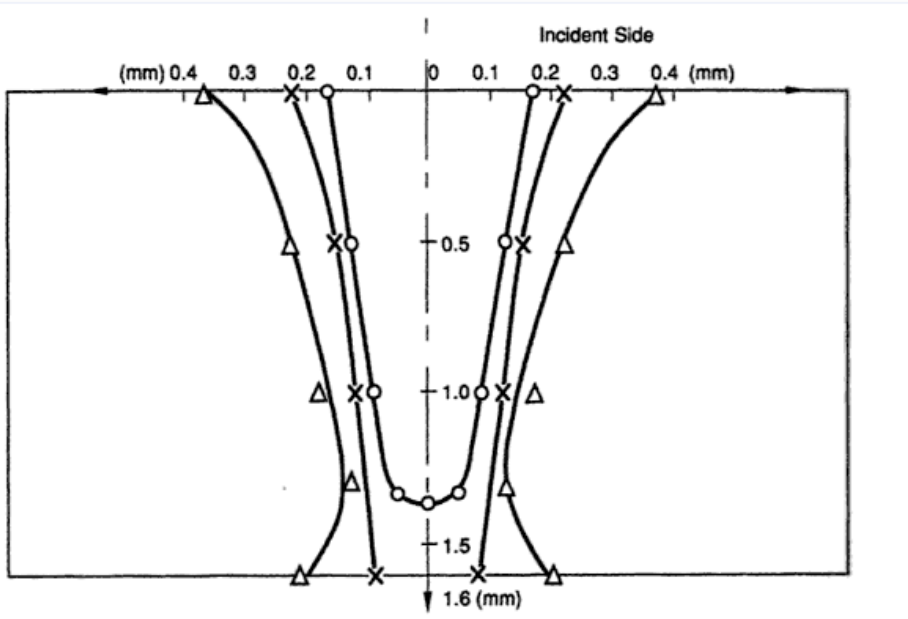

Figure 4: Cross section of holes cut with CO2 laser clearly demonstrating attenuation with depth [23]

This means all channels etched with the laser will have the same shape and that cutting through the material requires removing more material on the near face than on the far face.

1.5.2 Vaporization and Ejection of Molecules

When the light energy contacts the material, the energy first goes into breaking the bonds and melting the plastic. Once the plastic has been melted, the energy causes the material to eject. Due to rapid expansion of heated gases, the ejected material is deposited across the surface of the chip, sometimes falling back into the channel, but mostly onto other regions of the chip, as can be seen in figure below.

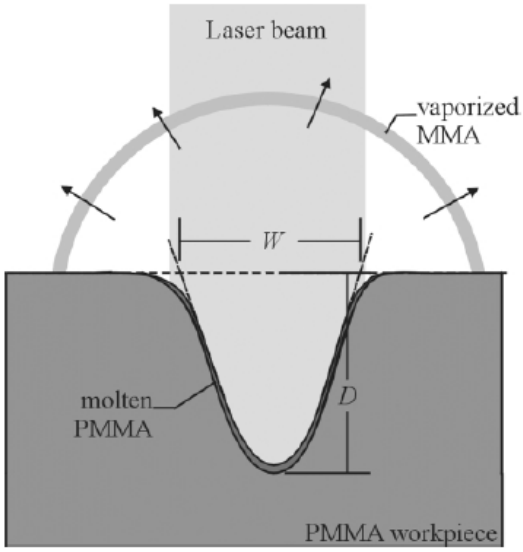

Figure 5: Schematic diagram of laser beam creating molten PMMA and a cloud of vaporized MMA [24]

Additionally, the melted material is pushed up the wall and creates a lip on the edge of the channel. The degree to which the laser penetrates the material is dependent upon the material's bond strength[25]. The depth of the penetration is also controlled by the speed and power setting supplied to the laser. The higher the amount of power and the slower the speed that the laser moves, the deeper the laser cuts. For example, a pass that is cut at 5 percent power and 10 percent speed will be shallower than a pass cut at 10 percent power and speed and deeper than a pass cut at 5 percent power and 15 percent speed. The ejected material from these cuts is detrimental to imaging the chip and potentially its functionality. However, the material does provide a benefit to sealing the channels as the deposited material and extra material pushed up to create a lip ensures that the channel is fully closed off when a cover is applied. For this project, polymethyl-methacrylate (PMMA) was used and thus hydrogen bonds and the bonds between monomers were the bonds broken during the cutting process. Thankfully, the thermal conductivity of PMMA is relatively low and therefore, as the laser

performs the operation, the depth of cut is very consistent because the material does not warp during the process. However, some inconsistencies have been noted at the start and end of cutting a channel. This is likely due to the mechanics within the laser system.

Another project within the Cal Poly Biofluidics Group found that a power setting of 5 yielded a channel with a width of 319 microns and a depth of 148 microns [26]. Since this width is considerably greater than 25 microns, or the step size, we can assume the channel should be fairly consistent.

1.5.3 Directionality of Laser Cutting

When cutting two intersecting channels, it is important to design which channel is cut first. As previously discussed, the laser deposits material on the lip of the channel as well as ejecting material. If the intersection is cut in the wrong order, it can lead to blockage or excess material in one of the channels. As can be seen in figures below, the final channel produced after engraving can vary depending on the manner in which it is cut. In the figure on the left, the extra heat from the last cut and the start of the new cut causes melting. The figure on right demonstrates how the horizontal channel was blocked by melted material from the diagonal cut.

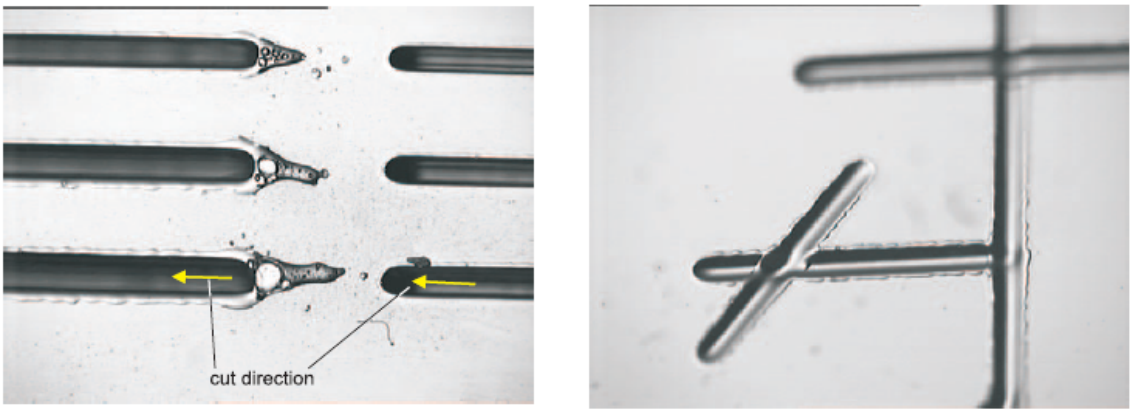

Figure 6: (Left) The extra heat from the last cut and the start of the new cut causes melting (Right) The diagonal laser cut has caused melted material to block the prior horizontal cut [27]

While these results may have no effect on the functionality of the chip that is dealing with small analytes, like ions, they have the potential to cause problems for larger molecules and in shallower channels. Additionally, obstacles such as these are capable of significantly altering the manner in which liquid flows through a channel. In Tim Abram's thesis, obstacles were used as a passive mixer to cause flow streams to cross one another under laminar flow conditions [10]. Furthermore, the additional surface area can cause issues with protein absorption and create pockets where flow becomes static, a biofouling issue.

The laser system functions similar to a standard printer in that it can be told to cut in raster form, oscillating side to side like a printer head, or vector form, which follows specified lines. Each of the primary colors can be given their own power speed and PPI setting. Therefore, a through-cut hole can be drawn in black, while a channel to be etched can be drawn in red. This color differentiation also dictates the order in which the channels are cut. Proper design will ensure that no intersecting channels are cut in the wrong order by specifying the correct color. As well, the more power-intense cuts and the cuts that will eject

the most material can be performed first in order to reduce the amount of ejected material that lands in the critical fluid channels.

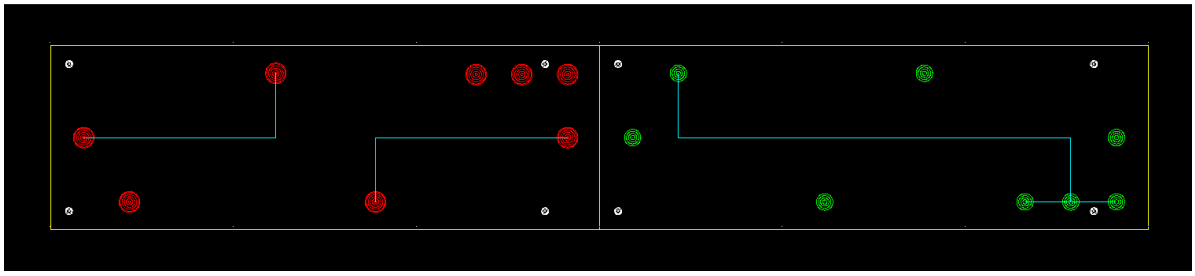

Figure 7: Example of CAD drawing used for laser cutting and engraving. Different color layers can be used to vary laser power and speed settings

Microfluidic chip designs can be created quickly using AutoCAD or any other CAD software. The precise dimensionality provided by CAD makes lining up through holes for interfacing and multiple-layer chips fairly simple.

1.6 Filter Processing

1.6.1 How it works

When introducing an electric field to draw ions out of a solution, a method must be introduced to prevent also removing other analytes of interest, like proteins. Since proteins and most other molecules carry a small amount of charge, they will be affected by an electric field and thus they each have their own electrophoretic mobilities. Since ions are highly charged for their size, they are the most affected, but removing any of the analytes, even if to a lesser extent, can interfere with downstream analysis. In this chip we used a physical barrier in the form of filter paper to prevent molecules larger than ions from crossing from the flow chamber to the electrode / waste chamber. As well, given that our separation method involves

the use of high voltage electrodes in direct contact with the fluid, electrolysis, or the formation of gases at the electrode, is a potential problem. The filter we used also prevented any bubbles from crossing into the flow chamber and interfering with downstream analysis.

1.6.2 Ion as Charge Carriers

Anytime the electrical conductivity of biological fluids is analyzed in literature the concentration of ions in the fluid is analyzed [28, 29]. This is because the ions are the primary charge carriers in a fluid and measuring their concentration in a given volume can be used to determine that solution's conductivity. For this reason, and their electrokinetic properties, they have become the chosen target analyte for this project. Since removing even a small percentage of the ions from a sample will significantly reduce the conductivity, we feel that reducing the conductivity of a sample by an order of magnitude is best done by using this approach. Since the conductivity is essentially a ratio of the charged solutes to solvent, the only other approach requires increasing the amount of solvent which is not as desirable in a microfluidics chip.

1.6.3 Case Study

In a study by Moorthy J. et al., several different filters were employed to create a microfluidics platform that was used to detect botulinum neurotoxin directly from whole blood [30]. The first of these filters was used for the purpose of sample preparation similar to the way in which the filter will be used in this project. The polycarbonate filter membrane contains 8 micron pores and is sandwiched between the two layers of base polymer material (PDMS) and serves to separate blood cells from whole blood. The filter serves to hold the

blood cells in a specific region of the chip while the rest of the sample continues to flow through the chip.

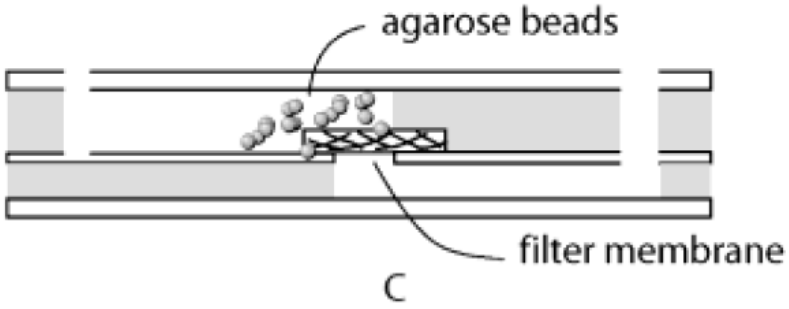

Figure 8: Side view of filter sandwiched between the two layers [30]

This approach demonstrates a two layer technique that is appropriate for use in this project to seal and hold a filter membrane that separates ions from the sample. Additionally, this paper works with raw, whole blood and demonstrates an analysis on chip. In other words, the chip successfully takes a raw sample, as would be taken in a POC application, and can perform pretreatment of the sample to the point that the sample can then be analyzed for the target analyte. This project could be integrated into a similar system and perform in a similar fashion to the filter used here.

1.6.4 Biofouling / Other Issues

One of the biggest issues in using a filter membrane to separate ions from the rest of the solution is that of biofouling. Biofouling refers to when the solids or larger molecules in a solution cause clogging by adhering and building up on the surface of the channels. This is of particular concern with a filter since the pressure-driven flow and electrokinetic forces drive the molecules towards the filter surface and can easily lead to an accumulation that clogs the

filter and ceases its function. When small sample quantities are involved, as is common in most microfluidics, rare proteins and other molecules lost to non-specific binding or biofouling may result in a critical error in analysis [31]. To combat this problem, proper chip design can aid by allowing flow rates to be high enough that it is difficult for the molecules to adhere to surfaces. Higher flow rates require chip sealing that can withstand higher pressures since moving more fluid through the same area will increase the pressure exerted on the walls of the channel and their seals. Additionally, the functionally of the chip can be impaired by a higher flow rate if not properly designed. In this particular case it is important to maximize the amount of area that the ions must diffuse through as well as the time they spend in the electric field. However, one other member of the Cal Poly Biofluidics Group is also working on a device that uses dielectrophoresis to prevent clogging of a filter that could be of use to future projects if these design constraints cannot be met.

1.7 Restatement of Project Goals

After discussing the significance of LOC technologies and the benefits of POC medicine, the importance of on-chip pretreatment should be clear. With background theory on electrokinetics, the use of filters, and the importance of ions in the electrical conductivity of fluids, the approach this project takes to lower the conductivity of biological samples effectively without removing molecules of interest should be clear. This project entails the design, manufacture, and testing of a PMMA microfluidics chip to remove ions with a combination of overcharged electrodes, dilution, and filtration. This project is considered a success if the conductivity of mock physiological solutions is reduced by an order of magnitude within five minutes.

II Materials and Methods

This section is intended to describe in detail the manufacturing techniques and equipment that was used to produce the microfluidic device used in this project. Many of the techniques that were used originated as methods that were developed by other projects within the Cal Poly Biofluidics Group or by other researchers found in the literature. Since the aim of this project was to develop a chip that proved a concept, most manufacturing decisions were directed toward creating a chip that was simply functional, not one that was sophisticated or anywhere near the limitations of this approach. Additionally, the chip was created as inexpensively as possible with the resources at hand, since the POC aim of this project requires such chips.

2.1 Microfluidics Chip Material Selection

In recent years, a debate has ensued over which materials are the best for fabrication of MEMS and microfluidic devices. One material that has shown significant promise is PMMA or poly (methyl methacrylate), due to its low cost and the ease with which it is handled. However, PDMS or polydimethysiloxane, has long been the staple of microfluidics research and thus many are hesitant to switch materials. However, PMMA has several key characteristics that are superior in comparison to PDMS with regard to its application as a microfluidic material. These include its increased structural properties, which allow for larger fluidic channels, and that it can be fabricated without the use of caustic chemicals and sophisticated equipment. Furthermore, PMMA is widely used in the manufacturing industry

for other applications and has the stiffness, strength, and durability to be used in clinical, non-prototype, settings. PMMA has been micro-fabricated effectively in many different ways, including photoablation, hot embossing, x-ray lithography, plasma etching and UV patterning. Photoablation is one of the most promising because it requires the least amount of expensive equipment and can create chips very quickly. However, PMMA is not without its obstacles. One of these major obstacles is chip sealing. It is difficult to create a watertight seal around PMMA microfluidic channels without deforming them, introducing contamination, or altering surface properties. Yet, several solutions have been published recently such as solvent and vacuum-aided thermal bonding [32]. Due to these recent advances and its industry potential, PMMA is poised to become the new dominate polymer substrate in microfluidics. For a more in-depth discussion of materials selection, please refer to Appendix B.

2.1.1 PMMA Sealing Methods

One of the major obstacles facing widespread use of PMMA is a lack of a simple yet reliable sealing technique for creating enclosed microchannels [33]. In other words, once the channels are made in the base piece of PMMA, it is difficult to then place a water-tight lid on the base piece such that the microchannels are not compromised or do not leak. Since PMMA is not a soft material like PDMS, it can be difficult to join a base piece of PMMA to a separate lid piece completely without having sealing issues, introducing contaminates into the chip, or deforming the shape of the channel. Some people work around this issue by either using a different material to join the pieces or a different material for the lid entirely. However, this

can have negative effects on the flow conditions in the microchannels by created regions of different zeta potentials and hydrophobicity.

The techniques used in literature thus far have included thermal bonding in a convection oven or in water, bonding with heated weights, thermal lamination, adhesive tape, a glue layer, and PDMS films [33]. However, Chen et al. suggests that thermal bonding is most desirable since it allows microchannels to have uniform surfaces of only one material. To address some of the problems of thermal bonding, such as microchannel deformation, this paper uses a thermal bonding process involving a vacuum. The vacuum heating oven was used at 112 °C for 60 minutes at a pressure of 10 millibar, which led to a tight interface between the two PMMA pieces. Given the relative simplicity of thermal bonding, this approach was attempted in this project and will be outlined in further detail later.

One of the more recent papers, Sun et al. [34], describes a new manufacturing technique that makes use of acetonitrile, a polymer-softening solvent, in combination with an SU-8 mold to create microchannels. This technique is novel in that it greatly shortens the manufacturing time for a PMMA chip to approximately fifteen minutes. It also provides a mechanism to seal the chip since a cover of PMMA can be softened with the same solvent and pressed into the base creating a bonded seal in thirty seconds. However, this project sought to keep costs and procedures simplistic and found this approach to be beyond the scope of this project.

2.2 Chip Design

2.2.1 Precursor Chips

The start of this design began by looking at other designs from the Cal Poly Biofluidics Group that were precursors to this project. The first of these was also the motivation for this project, as this project aims to address issues discovered in Tim Abram's project [10]. His pretreatment chip used buffers and micromixing to successfully treat bovine calf serum for pH and viscosity. Viscosity and pH are equally important parameters as conductivity for the success of downstream analysis. However, his chip was unable to reduce the conductivity of the serum using micromixing due to dilution issues. Mixing buffer with serum to lower the serum's conductivity was dependent upon the relative volumes of the buffer to the serum. To lower the conductivity sufficiently required mixing a very large volume of the buffer with the serum and was essentially not feasible given his chip design. Thus, the method used by this project to treat conductivity was developed. Abrams's work served as inspiration in terms of the importance of on-chip pretreatment and successful chip design for such aims.

The other source of inspiration from within the group was the work of Evan Barbre [26]. Barbre's work focused on developing a successful capillary electrophoresis chip using PMMA and laser processing. The manufacturing techniques developed in his thesis using our in-house equipment well characterize the manufacturing techniques used in this project. As well, without his work this project likely would have been done in PDMS instead of PMMA as the group lacked the equipment and expertise to use PMMA prior to his thesis.

With these two sources of inspiration, a design was created that took into consideration the major criteria. The first of these was a method to create an electric field on chip. Second, the design would needed to account for the scale difference of the features to the relatively macro scale size of the filter membrane. Third, the removed ions should go to a waste reservoir, while the treated sample would need to be sequestered in some manner so as to have its conductivity measured. And fourth, the directional requirements of the electric field were such that it needed to be directed through both the sample and the filter membrane so as to remove the ions.

2.2.2 Design Constraints

The first of these constraints, establishing an electric field, required implementing electrodes into the design that could be wired to a voltage source. Since the fabrication of this chip was intended to be done inexpensively and without the aid of a clean room, this project used the electrode design developed in Evan Barbre's thesis. This involved wrapping a 23 gauge hallow metal tubing, or hypo tubing, with electrode wire and inserting the hypo tubing into Tygon® tubing which interfaced with the chip (see Figure 9). Thus, the electric current travelled from the electrode wire to the hallow tubing, into the fluid within the hypo tubing, down the Tygon® tubing and into the chip only to return through a similar apparatus. While not as elegant as some solutions, such as contactless conductivity detection [11], this solution is inexpensive and allows for rapid production of functioning chips for prototyping.

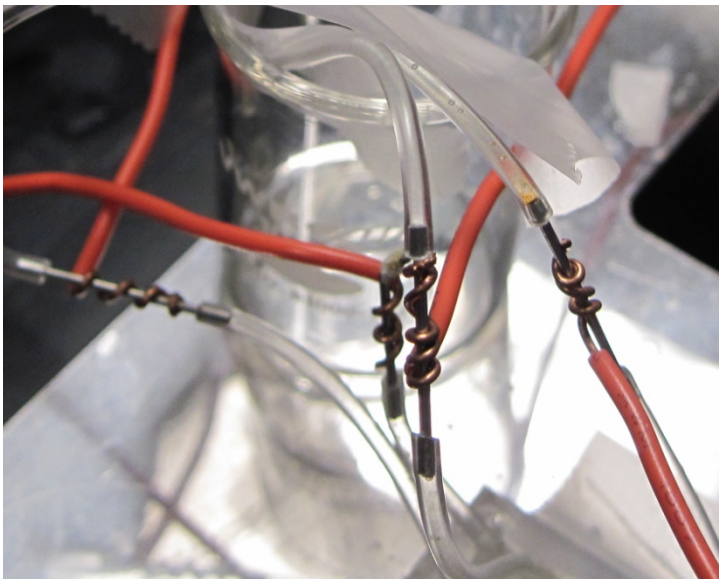

Figure 9: Electrical wire is wrapped around hallow stainless steel tubing and inserting into the interfacing Tygon® tubing allowing current to flow

The second constraint involved designing a chip that incorporated both features on the scale of several hundred microns and a filter membrane that was previously fabricated and of a much larger size. After several designs it was discovered that this constraint could only be addressed with a multilayer chip. In other words, attempting to fabricate a device with this constraint that existed entirely in a single layer of PMMA with our limited resources did not seem feasible. Thus, the simplest solution was to the design the chip to incorporate two PMMA layers with the filter membrane sandwiched between them. Much like a clamshell, this design allowed for the filter handling to involve only cutting it to a proper size and placing it between the two pieces.

To ensure that the electric field pulled ions through the membrane, the design required that the electrode channel be separated from the sample channel by the filter and that the positively and negatively biased electrode channels are oriented such that the electric field

had to pass through the sample channel. In the original design, this was accomplished using the layout seen in the figure below.

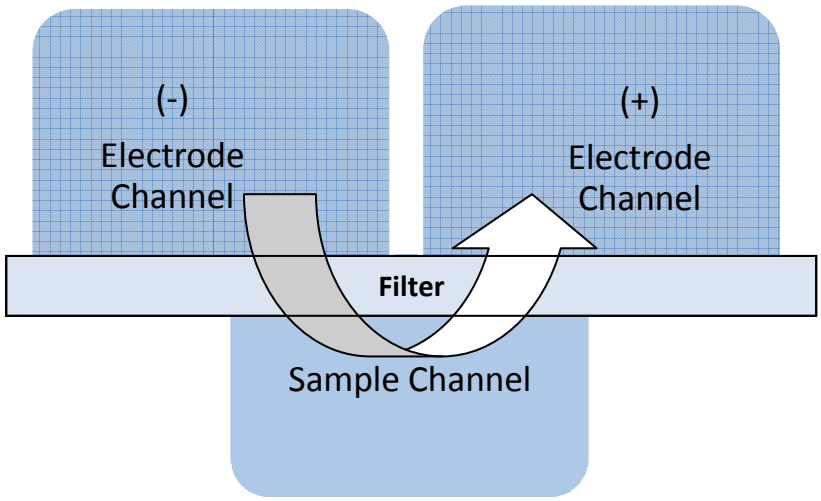

Figure 10: Cross Section Diagram of Channel Layout Design

From this cross section diagram you can see that this design separated the electrode channels with PMMA such that the electric field had to flow from one electrode channel, through the sample channel and into the other electrode channel. This caused ions flowing along the sample channel to be attracted toward the ceiling of the sample channel and into the electrode channel of opposite charge. One drawback to this design, however, was that it required proper alignment of the top and bottom pieces and sufficient structural integrity of the small amount of PMMA separating the electrode channels. This will be discussed in greater detail later.

To keep the ions separated from the sample, the electrode channels had to remain separate from the sample channel and from each other. Therefore, two waste outlets were designed

into the chip, one for each of the electrode channels. As well, the sample channel required its own outlet where aliquots could be taken if needed. In total, three inlets and three outlets were required for this design.

However, for the last design constraint of measuring the conductivity, it was decided that real-time measurements would be ideal and that the chip should incorporate the ability to measure conductivity on chip. To accomplish this, two additional outlets were added on both sides of the sample channel outlet to allow another electric field to be created that ran through the outlet region of the sample channel (see yellow reservoir illustrated on the right side of Figure 11). This would allow for measuring the conductivity of the sample without having the other electric field on. However, it was discovered that having three outlets in parallel resulted in the fluid taking the channel of least resistance or the shortest tubing. Thus, even minor differences in tubing length resulted in the outflow moving almost entirely through one channel and not the others. This ultimately led to the creation of poor data. Additionally, voltage or current measurement taken while the other electric field was engaged was significantly affected and also resulted in poor data. For this reason, all data measurements were eventually taken off chip.

2.2.3 Geometry and Drafting

Most of the chip layout and design work was done using AutoCAD 2010. This software is useful in design of chip layouts since precise locations, distances, and geometries can be created such that when the chip is produced, a very accurate result is achieved. This software is of particular use with the CO_2 laser cutting machine, since the files can be read directly by the machine's software drivers. The Universal Laser Systems' plotter driver is capable of

tracing lines drawn within an AutoCAD drawing to within 25.4 microns [22]. As mentioned prior, the plotter driver also allows for separate programming of power, speed and pulses per inch (PPI) based upon a line or hatch color. Since AutoCAD is capable of modifying line and hatch colors simply by changing the layer on which they are drawn, the power, speed, and PPI can also be easily controlled with this feature.

2.2.3.1 Geometry of Initial Design

The first design created took advantage of the cross section shown in Figure 10 as a method to separate the channels by the macro scale filter, while also creating the desired electric field through the sample channel. The top view layout of the two layers and the drawing created in AutoCAD can be seen in the figure below.

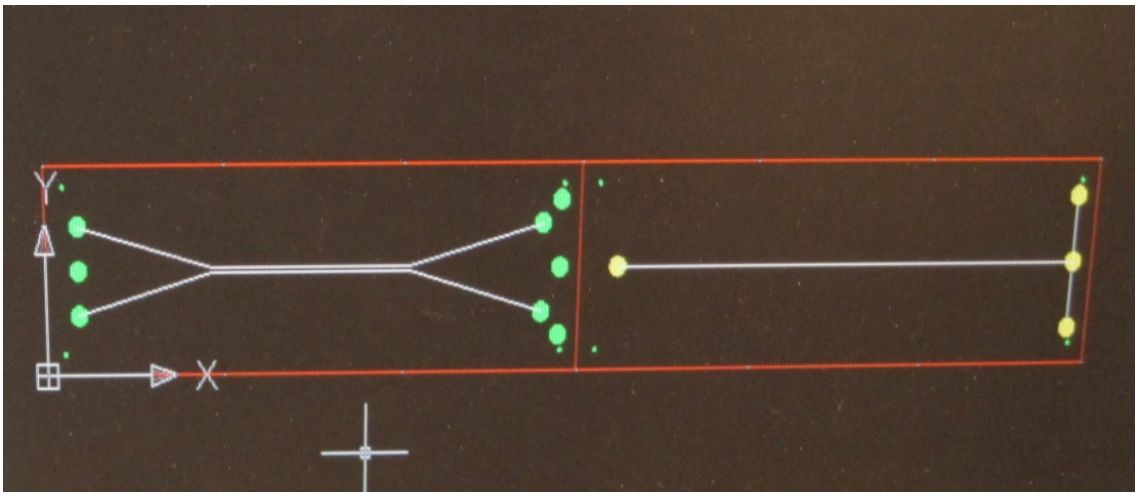

Figure 11: Initial AutoCAD design. Channel lines to be engraved shown in white, through cut lines shown in red, through holes shown in green and reservoir holes shown in yellow. Electrode channels are shown on the left, the sample channels are shown on the right

The design incorporates having to sandwich the filter between the two layers of etched and cut PMMA. This was the only approach that was feasible given the size of the filter that was to be incorporated into the chip. However, having these two pieces sandwich the filter in a

clamshell-like fashion produced some interesting considerations. The first of these was that the chips needed to be aligned so that the channels matched up from one piece to the other. Without lining up the pieces accurately, there would be no interface between the electrode channels and the sample channel. A possible outcome of such a misalignment is illustrated in the following figure.

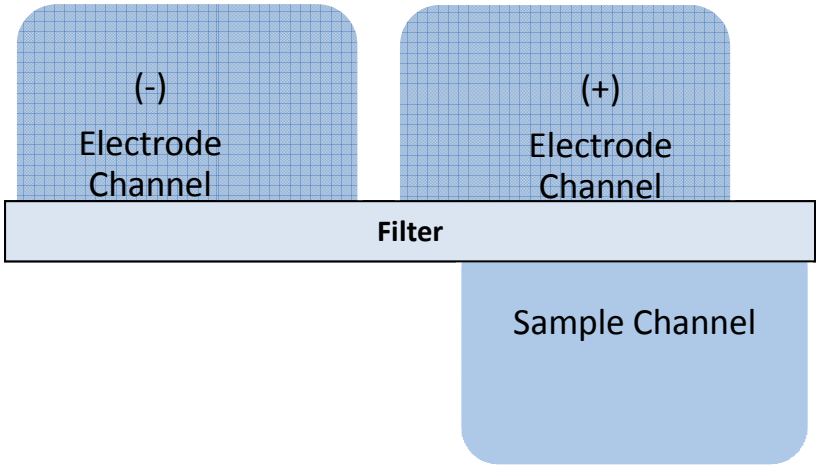

Figure 12: Misaligned channels result in chip that no longer functions

To compensate for this issue, later designs incorporated holes cut into each of the chips in key locations such that when these holes were lined up, the chips would also be lined up. The holes were designed to be small and work with the same 23 gauge hollow metal tubing used in the electrodes, which can also be found on the end of some syringe tips as can been seen in Figure 13. With the tubing inserted through the alignment holes on both chips in multiple locations, the accuracy of the laser cutter essentially becomes the accuracy of the alignment.

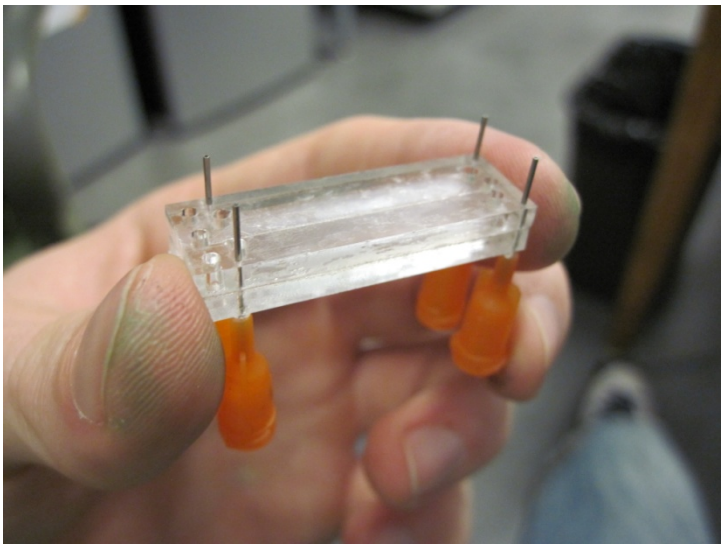

Figure 13: Syringe tips function as alignment rods to line up the two pieces of PMMA and their channels

The other issue that presented itself as a result of the clamshell design was that access to the channels would have to be done through the thickness of the PMMA both in terms of interfacing and imaging. Most single layer chips designed in our research group and in literature involve the use of a glass slide and PDMS such that the features on the chip are located on the bottom of the chip just above the glass (see figure below).

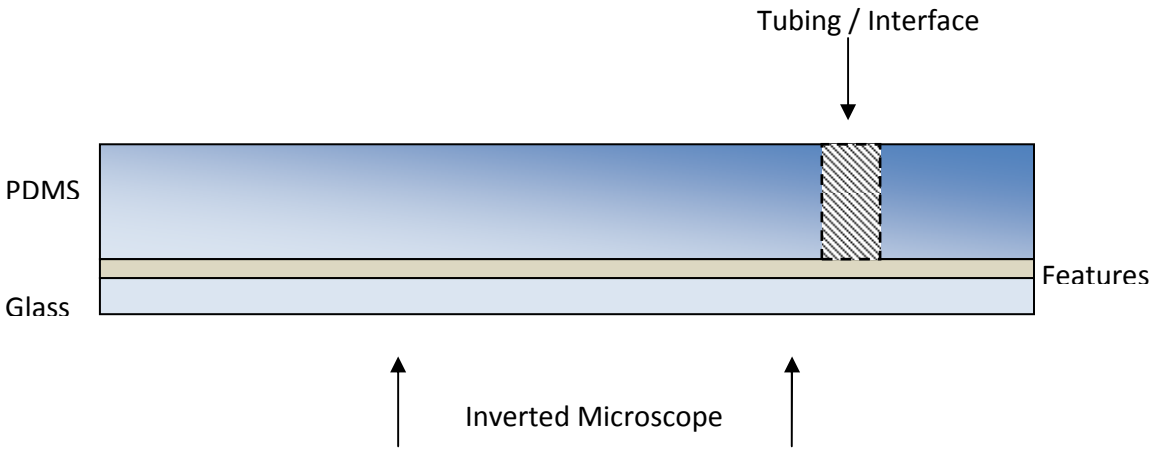

Figure 14: Schematic of feature placement for imaging on typical PDMS chips

This allows inverted microscopes, like the Labsmith SVM340 used in this project, to have to focus only through the glass. The interfacing done with tubing, syringes, and electrode wire can then be connected through the top of the chip so as to not interfere with the imaging. With this clamshell design, the imaging must be done through the PMMA piece on the bottom and through the bottom of the features, or the channels that have been ablated. The PMMA is considerably thicker than a glass slide, is not as optically transparent, and is scarred by the laser etching, as demonstrated by the figure below. Because of this, much of this project had to been done without being able to visualize the functionality of the chip.

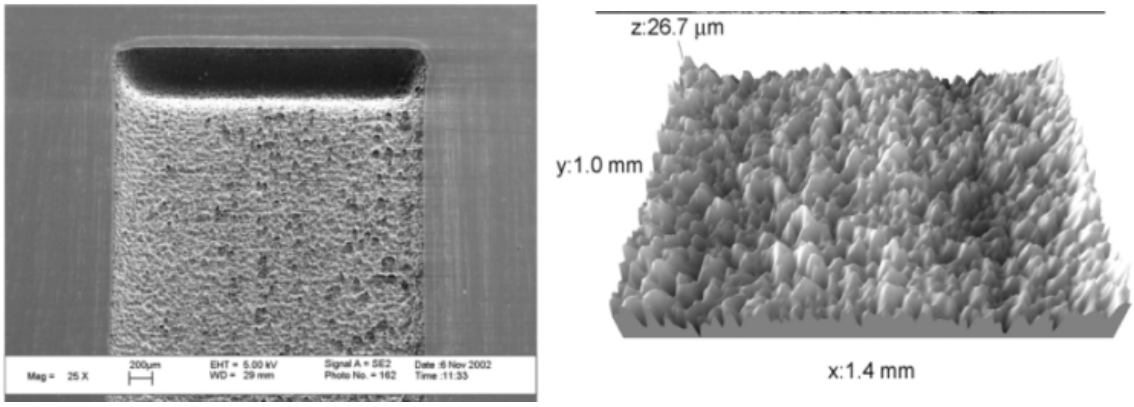

Figure 15: Surface roughness of PMMA after laser etching [35]

If future researchers are capable of producing a design that does not require this clamshell approach or can find a better way to image the channels, this design should be avoided. However, since the success of this project hinges on quantitatively measuring a change in conductance rather than observing a process, this design can be used even without the imaging.

2.2.4 Laser Manufacturing

Most of the time spent manufacturing the device was spent working with the laser system located on campus. The laser is located in a machine shop that is open to public access provided you are a student of Cal Poly and pass the required safety test. This is important to note since the day-to-day consistency using the machine was very low as a result of the numerous people that used the machine. Additionally, such a machine requires fairly regular maintenance to keep it running properly and as efficiently as possible, a requirement which was likely not done enough given the amount of use the machine receives. Thus, the parameters developed for cutting and rastering should only be taken as rough settings that need to be tweaked each visit to achieve optimal results. The manual included with the laser system provided recommended settings for cutting and engraving acrylic, which are given below.

Table 2: Recommended settings for laser cutting found in the system's manual [22]

Operation	Wattage	Power	Speed	PPI	Depth (inches)
Vector Engraving	60	2	4	1,000	0.005
Vector Cutting	60	100	2	1,000	0.250

While these settings were a good starting point, they weren't established for microfluidic devices. Instead a better starting point were with the settings described in Evan Barbre's thesis [26]. Evan used settings that were more similar to the following:

Table 3: Recommended settings for laser cutting found in Evan's thesis [30]

Operation	Wattage	Power	Speed	PPI	Depth (inches)
Channel Engraving	60	5	10	1,000	Approx .006
Cutting Chip out of Stock	60	49	3	1,000	Through Cut (At least 3/16)

Theses setting were refined as the project evolved but formed a good basis for a microfluidics chip. The difference between these settings and those provided by the laser system manual were that for the channel, engraving a shallower and narrower channel was desired to maximize the effect of the electric field through the sample channel. Thus, the speed of the cut was increased to 10 from 4, more than doubling the speed. As well, to remove the chip from its stock material it was found that lowering the power to 49 and slightly increasing the speed was still a sufficient cut through the material, but also provided a chip that was less burned and cleaner than the higher power setting of 100.

2.2.4.1 Chip Interfacing

Since microfluidics chips are on a small scale, integrating the external requirements of the chip, such as the voltage sequencer to power the electrodes and the syringe pumps to move the fluids, can be difficult. This requires interfacing a small scale chip with larger scale equipment. Tygon® tubing was found to be one of the effective means to accomplish this goal in other Cal Poly Biofluidics Group projects. Tygon® tubing is flexible, stable, and is

nonreactive in almost all applications. The tubing used in this project was approximately 1/16 of an inch in outer diameter and 1/32 of an inch in inner diameter. The Tygon® tubing has the same inner diameter as the outer diameter of 23 gauge hypo tubing and syringe tips. These syringe tips luer lock with most standard syringes which can then be used with the Harvard Apparatus Syringe Pump. Placing the Tygon® tubing into the PMMA requires the hole be slightly smaller than the nominal outer diameter of the Tygon® tubing. As can be seen in the figure below, the laser power attenuates the deeper it goes and therefore the holes that are cut for interfacing are smallest at the top.

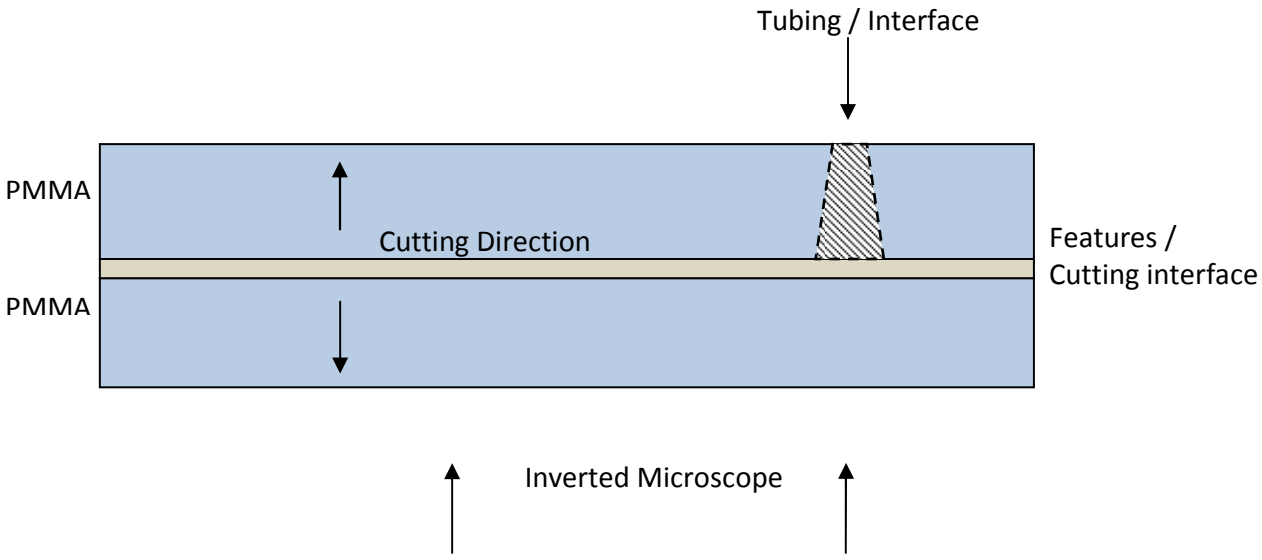

Figure 16: PMMA clamshell design where through cut holes attenuate with depth. The cutting surface for both pieces of PMMA can be found in the middle of the diagram

By using a pair of tweezers the Tygon® tubing can be squeezed into the hole such that the top of the hole holds the tubing in place. This keeps the tubing from coming out of the hole or moving too deeply into the hole, causing the flow to be blocked by the PMMA below. Tubing was cut such that the syringe pumps and the electrode connections could

conveniently be hooked up to the chip, but as short as possible so as to lessen the amount of fluid that would have to be dispensed to clear the system after experiments. Generally the total length of tubing, from the syringe pump to the electrode location and finally to the chip, was around six inches. As described prior, the electrode wire was wrapped around 23 gauge hollow stainless steel tubing that had both ends inserted into Tygon® tubing as shown below. The stainless steel tubing was cut to be approximately a cm in length by using a razor blade and rolling the tubing under pressure from the blade along a flat surface. This technique ensured clean cuts without metal being bent into the opening of the tubing as it was found that most clippers produced.

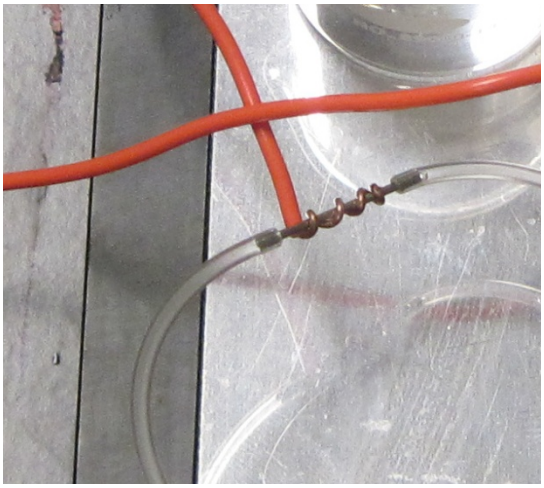

Figure 17: Electrode wire is wrapped around stainless steel hypotubing to create a conductive path from the voltage sequencer to the fluid

In order to seal the Tygon® tubing into the PMMA, a standard epoxy for acrylic was used. A small amount was mixed in a disposable weigh boat and was applied with the end of a syringe tip to the Tygon® tubing. A ring of epoxy was created about 1 cm from the end of the tubing, such that when the tubing was inserted into the hole in the PMMA, the epoxy formed a complete seal around the tubing. Using this method avoided much of the mess that

resulted from applying the epoxy after the tubing was inserted. However, special care had to be taken not to get any epoxy near the tip of the tubing as it would clog the tubing and/or the chip when it cured.

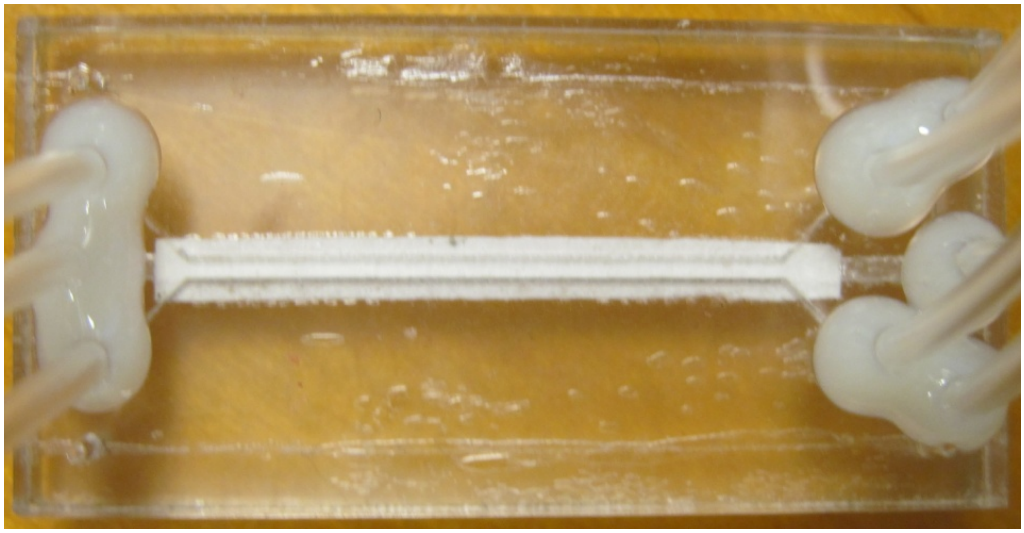

Figure 18: Tygon® tubing is inserted into the PMMA with a ring of epoxy near the end resulting in the cloudy circles seen here

Initially the through holes were cut out of the PMMA using a raster operation by the laser system. However, after some time it was discovered that the rastor processes took significantly longer to cut a chip than making the design out a series of vector passes. The figure below illustrates the difference in design between a raster and vector processes in AutoCAD.

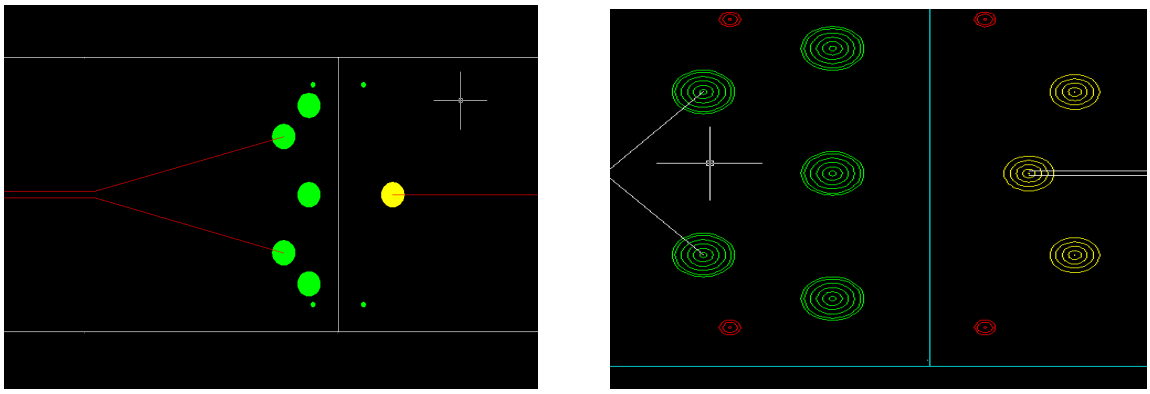

Figure 19: Hole design in AutoCAD. (Left) Solid Hatch translates to raster cutting on the laser system. (Right) Separate circular lines translate to vector cutting found to be more efficient

The laser settings for the two different designs were as follows:

Table 4: Laser setting for though hole cutting

Operation	Wattage	Power	Speed	PPI	Depth (inches)
Raster Cutting	60	62	3	1,000	Through Cut (At least 3/16)
Vector Cutting	60	45	3	1,000	Through Cut (At least 3/16)

The vector setting features a lower power setting than the raster since the raster process would move from hole to hole as it was cutting, allowing the heat to dissipate more completely than during the vector process. In a raster process, the laser head will move across the entire design in a horizontal, side-to-side motion, much like a printer head that crosses a whole line of text rather than writes each individual letter. The vector process, on the other

hand, moves from one drawn line to the next nearest separate line and will thus complete the cutting of a hole all at one time before moving to another hole.

2.2.5 Reservoir Design

As the first chips were being interfaced with Tygon® tubing, it was realized that the tolerance on the hole diameters designed to hold the Tygon® tubing were difficult to meet. Since the laser used to manufacture these chips is located in a relatively public machine shop, parameters had to be adjusted nearly every visit. This resulted in deviations in the final produced chip even when the same parameters were used from run to run. Test pieces were cut with slightly different hole diameters and then fit with the tubing to find the sizing that worked best. An example test piece can be seen in the figure below.

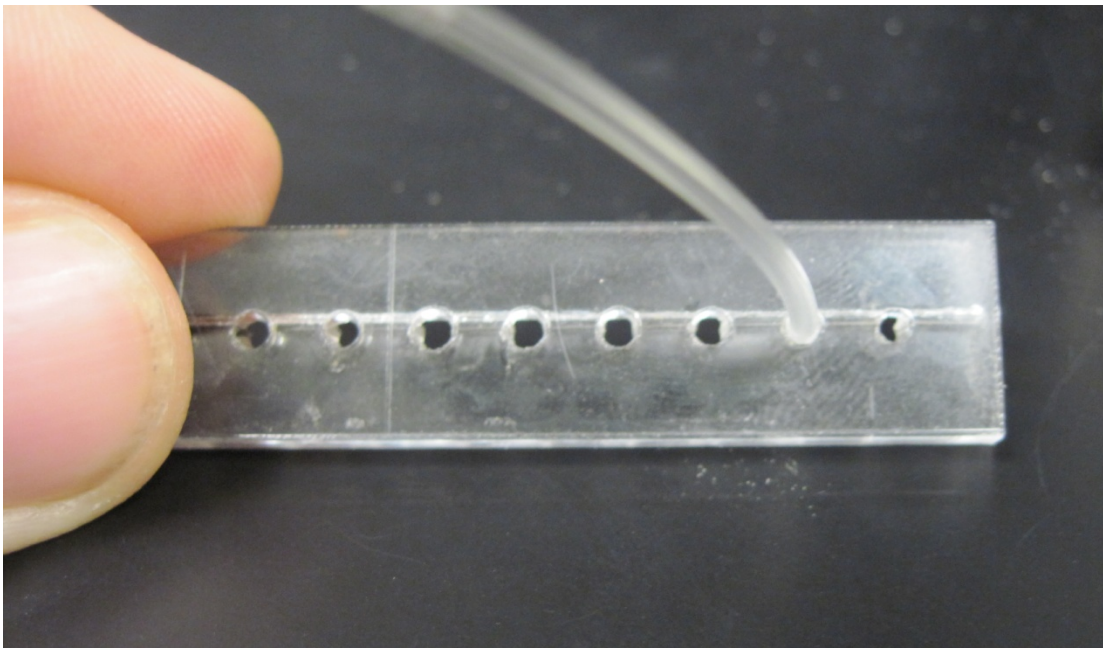

Figure 20: Test piece for hole diameter calibration

While this compensated for much of the deviations, to ensure that the chips could still be used it was important to incorporate reservoirs into the design. These reservoirs were holes that were cut into the lower piece of PMMA, but not with much power so that the holes only went a small depth into the PMMA. This pocket ensured that if the through holes for the Tygon® tubing were too large and the tubing slid deep into the hole, that flow would not be obstructed but could flow down into the reservoir.

2.2.6 Chip Bonding and Sealing

Unfortunately, this was one of the most difficult aspects of this project. PMMA can be bonded to itself through many different measures such as thermal bonding, adhesives, or solvents [36]. However, since this project uses a clamshell design, the chip required a sealing method that would not occlude channels on either side of the chip. Most solvents and adhesives were thought to cause problems in this regard and, thus, thermal bonding was the first sealing method attempted. During the bonding, the alignment method described prior was used to keep the two pieces of chip in the correct places. Additionally, clamps were used to apply pressure to the chips as they were heated (see below).

Figure 21: Clamps were used to apply pressure during thermal bonding of the chips

To test the success of the bonding and sealing, syringes were filled with water and food coloring and attached to Tygon® tubing. The Tygon® tubing was then inserted into each of the holes on the device and light manual pressure was applied to the syringe to inject colored water into the chip. This allowed visual conformation that fluid flowed from inlet to outlet without leaving the channel. A successful bonding is shown below with green food coloring acting as the dye.

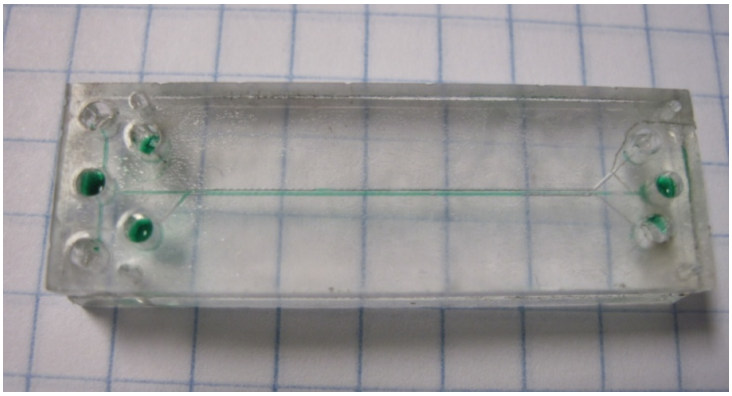

Figure 22: Water tight seal testing with green food coloring. Dye only being located in the channels indicates that this chip was successfully bonded

However, using only thermal bonding was quickly found to deform the chip, essentially warping the chip such that it no longer lay flat, or to not seal the chip at all. The difference between the two was the temperature and time allotted for the chip to bond. However, finding a successful set of parameters appeared to be impossible once the filter was introduced between the chips. The next solution involved what was thought to be a simple, inexpensive, and relatively easy fix that involved the addition of double sided tape to the sealing process. A gasket was designed in AutoCAD that had the same features as the chip design. This allowed the tape to be cut with the laser system. An example of this gasket design can be seen below.

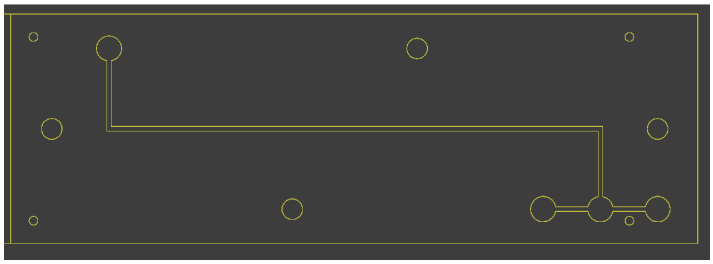

Figure 23: AutoCAD drawing of gasket design. Large areas are removed around features to prevent the adhesive from interfering

However, after cutting several pieces it was discovered that the tape would be very difficult to work with, as it adhered to just about everything. This made it very difficult to align to the chips without damaging the fragile tape. A tape with a backing was sought out to make handling easier, resulting in 3M's 9576 tape which can be seen in Figure 24. Despite being easier to handle, the notion of a gasket, which left excess room for the features, was further found to be an issue, as the thickness of the tape would allow for fluid to spread in those areas where the tape was not in place. Thus, if double sided tape was going to work, the tape needed to be the same dimensions as the features with which it was being used.

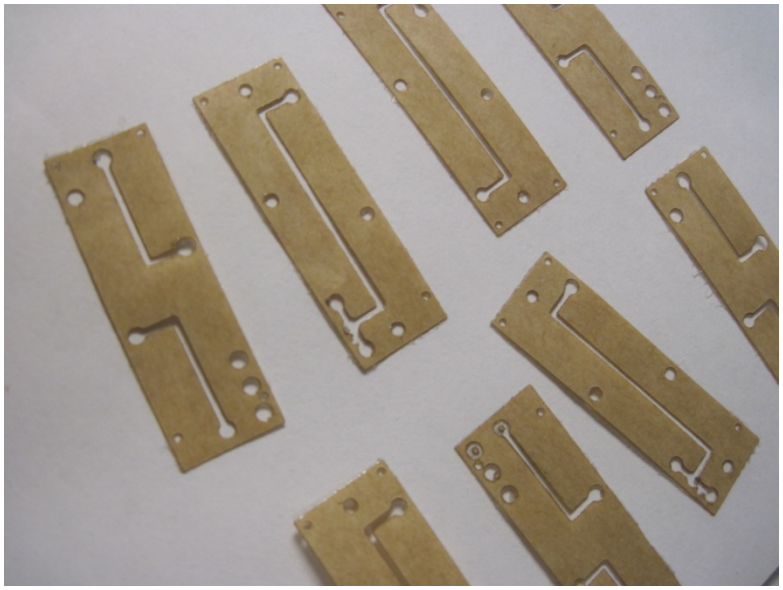

Figure 24: Double sided tape cut by the laser system shown stuck to a piece of paper for temporary holding

At this point the tape was then placed on the uncut PMMA and both the tape and the PMMA were cut together. This required increasing the power supplied to the laser by some degree to compensate for the additional thickness of the tape, as well as widening some of the dimensions to compensate for attenuation of the laser from the top of the tape to the bottom of the tape. The final product of these efforts can be seen in the figure below.

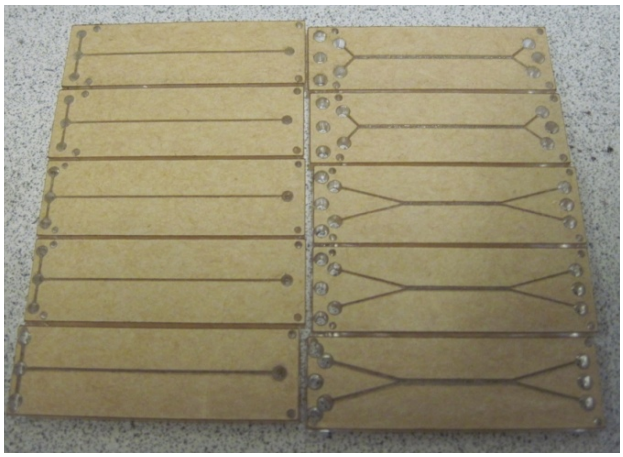

Figure 25: PMMA and double sided tape cut in a unified process by the laser system

These efforts allowed each half of the chip to have its alignment pins inserted, the backing removed, the filter inserted, and the chip pressed together with ease. This process is outlined in the figure below.

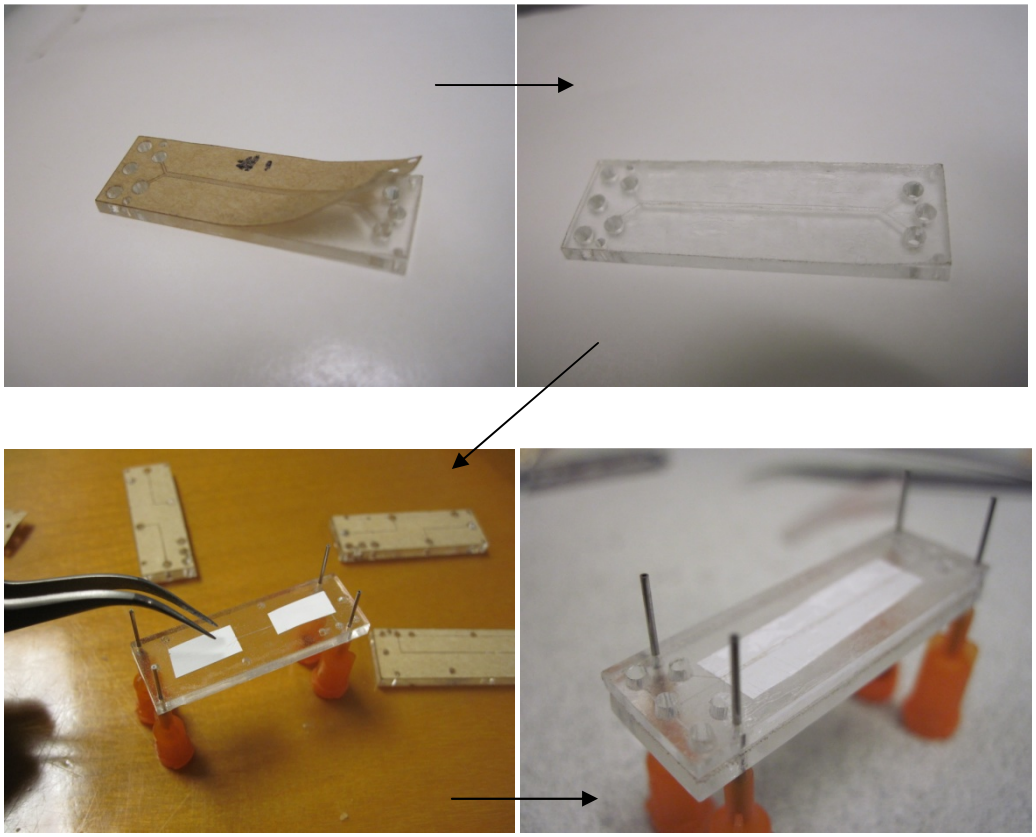

Figure 26: (Moving Left-Right, Top-Bottom) Backing is removed from each half of the chip, the alignment pins are inserted, filter paper is placed on one side of the chip, and finally the other piece is pressed on top

However, once the chip is assembled, a further thermal process was needed to keep the chip from leaking. Several different temperatures, times, and clamp locations were attempted with success only occurring when the filter was not placed between the two pieces.

The protocol used to heat the chip was modeled after the process used by Greer et al. [37] but modified to follow the findings of a peer in Cal Poly Biofluidics group. The settings for this protocol involved placing the clamped chip in a furnace for 20 - 30 minutes at 75 degrees

Celsius. While this approach appeared to be doing its purpose in sealing the two pieces of PMMA together, it appeared that the combination of heat, time, and pressure resulted in chips that, while sealed, were also clogged. While the combination of those three factors provided the adhesive enough energy to bond sufficiently to the PMMA, it also permitted sufficient energy for thermal expansion and melting. This resulted in adhesive melting down into the channel and clogging them (see figure below). This was a problem we tried to avoid previously by using a strictly thermal bonding process.

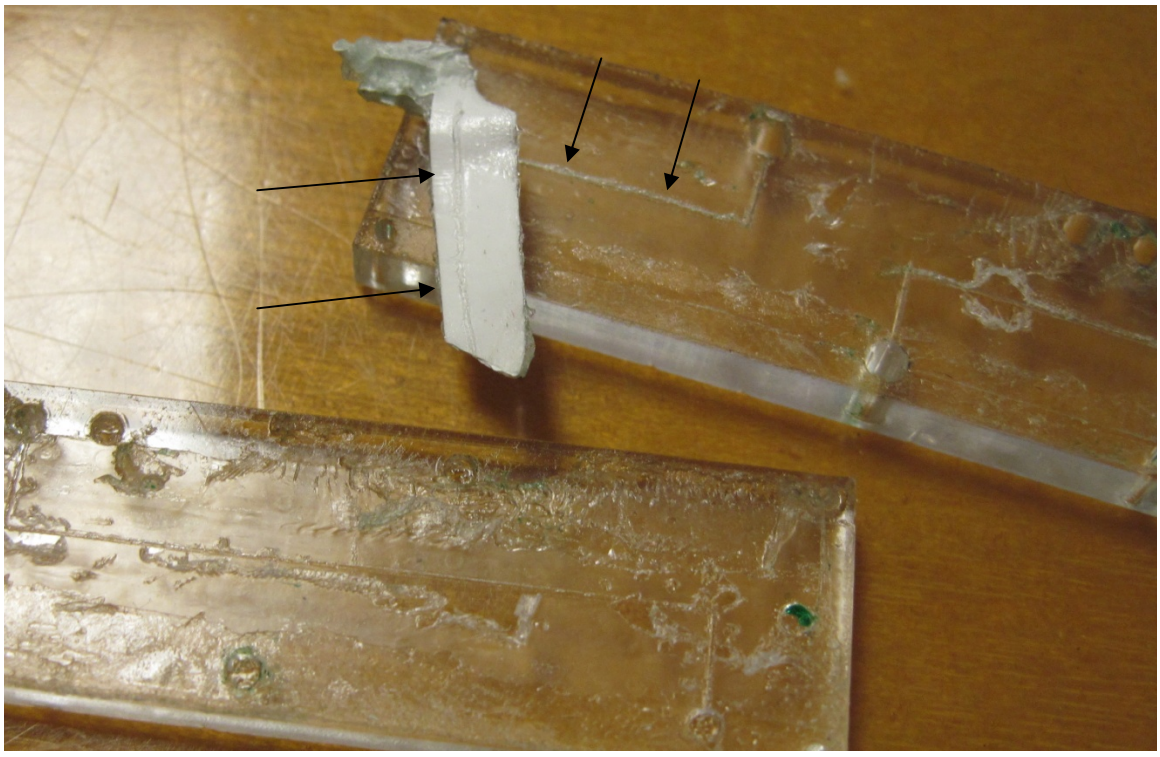

Figure 27: Chip pulled apart after sealing process reveals adhesive to have melted into the channels

Table 5, shown below, demonstrates the failed attempts at working around this observation and the need for a design change. Since this chip was aimed only at validating this approach to conductivity conditioning, we arrived at a solution to the sealing problem by widening the

channels. It was believed this solution could be implemented without negatively affecting the functionality of the chip beyond the tolerance of this project.

Table 5: The data below is from attempts at different sealing methods. This data determined that the channels needed to be widened to use this approach

Chip Number	Clip Presence	Filter Presence	Temp (C°)	Time (Min)	Observations
1	NO	NO	75	18	Sealed/Functional
2	YES	NO	75	18	Clogged
3	YES	NO	75	15	Clogged
4	NO	YES	75	14	Leakage
5	NO	YES	75	23	Leakage
6	NO	YES	75	30	Leaked (clipped during cooldown)
7	YES	YES	75	14	Clogged (attempted to remove excess adhesive prior to sealing process)
8	YES	YES	75	12	Leakage

2.2.6.1 Other Sealing Issues

At this time it was noted that the current design, which featured side by side electrode channels (see Figure 11), may not properly force the electric field through the sample channel. As a result of the laser ablation process, the PMMA that forms the barrier between the electrode channels was found to be warping. The warping can somewhat be seen in the photo taken by the video microscope below. Any damage to this material would allow both fluid and current to move freely from one electrode channel to another which results in an ineffective electric field.

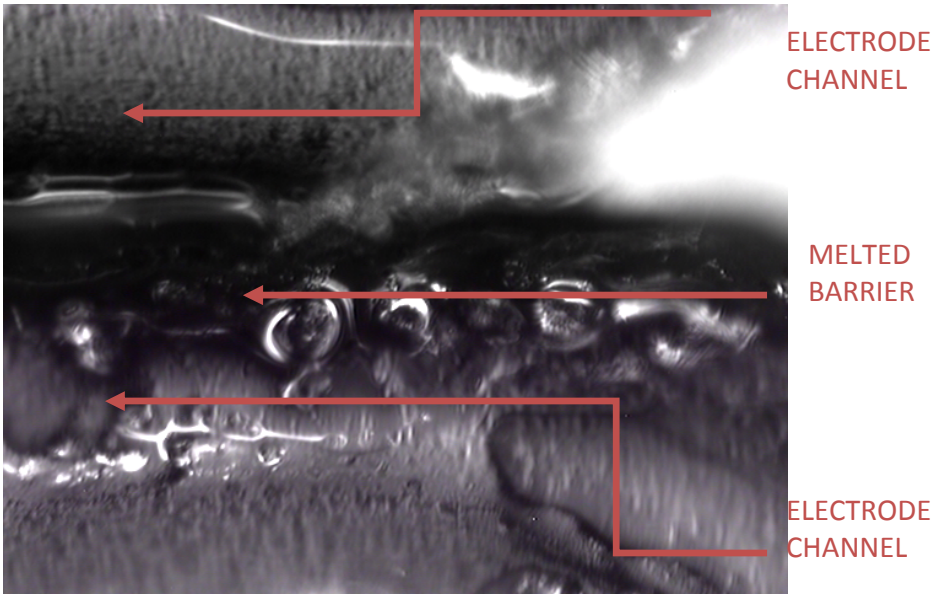

Figure 28: Image taken with video microscope demonstrating the warping of the material between the electrode channels

As a result, the chip was redesigned to eliminate this design flaw in two different ways. The first was to compensate by widening the sample channel and further separate the electrode channels. By separating the electrode channels, the barrier between them was further thickened, as well as its robustness. Additionally, it was thought the widened sample channel would increase the retention time. The second design used standard designs from capillary electrophoresis for inspiration. One of the electrode channels was moved downstream while the other was moved upstream so that they no longer connected in the middle (see Figure 29).

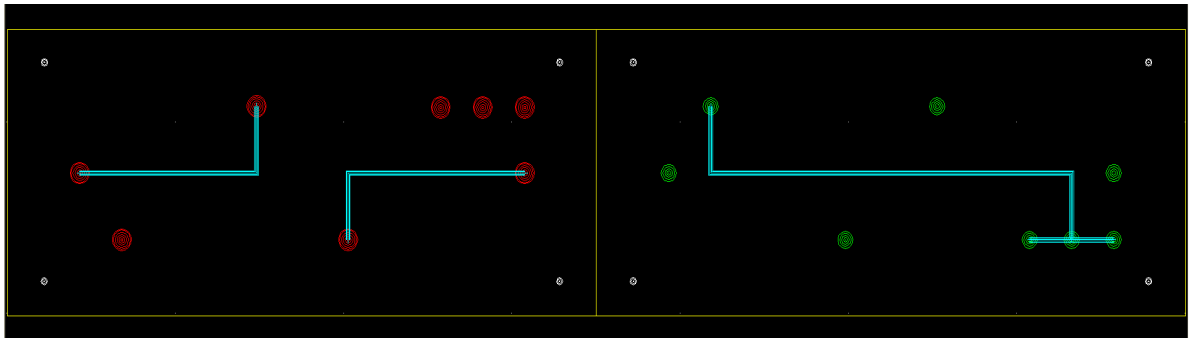

Figure 29: Final device design which separates the electrode channels up and down stream rather than side to side

The electric field was thus established parallel to the fluid flow rather than perpendicular as it was in the other design. Both of these designs were tested and their results will be discussed in the results section.

2.3 Modeling

Due to the relatively simplistic design used in this project there was not a need for extensive modeling. However, a limited amount was done using COMSOL to determine the path of the electric field as well as its strength in an idealized channel design.

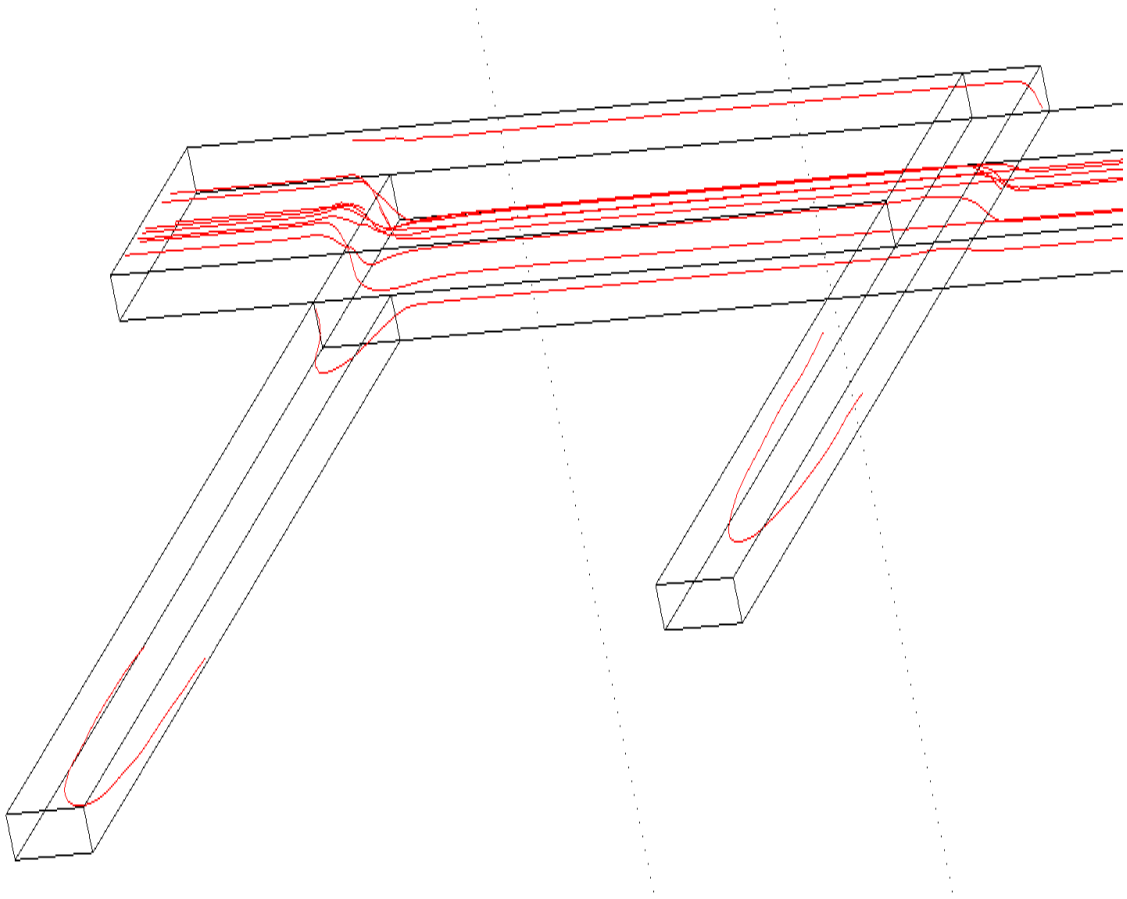

Figure 30: COMSOL model demonstrating the streamlines of the electric field in the microfluidic device. The electric field crosses from the one electrode channel to the sample channel and into the other electrode channel, as predicted

Using the stokes flow and conductive media DC models from the MEMS module in COMSOL, this plot was generated to show the path of the electric field in one of the chip designs. Of interest in this figure is the manner in which the electric field bends from the electrode channel, shown on top, into the sample channel, shown below it. This response is repeated at the other end of the chip not shown in the figure. This demonstrates that, theoretically, the electric field should travel from one electrode channel, through the sample channel, and into the other electrode channel, as predicted.

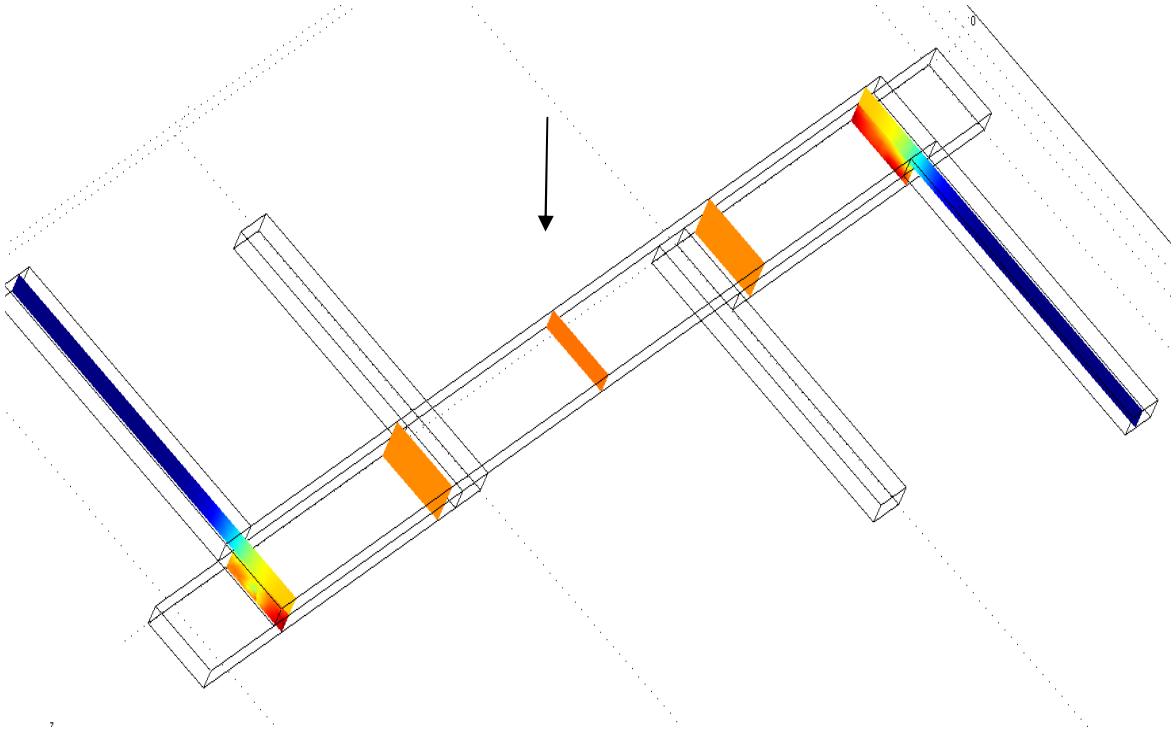

Figure 31: COMSOL model illustrating the magnitude of the electric field at five different slices within the fluid channels. The color indicates the relative strength of the field with red being the strongest and blue being the weakest

Another COMSOL model was developed to explore the strength of the electric field within the microfluidic channels. As can be seen in the figure above, the magnitude of the electric field is indicated by a color gradient. The red end of the spectrum is used in areas of high field strength while the blue end is used in areas of relatively low field strength. From this model it would appear that the electric field is strongest in the area indicated by the arrow. This agrees with what would be expected, as the field must pass through only the sample channel in this area. The field also appears to weaken in the sample channel proportionally with the distance from this midpoint. This is likely due to the field crossing from the sample channel to the electrode channels. Finally, the inlet and outlet to the sample channel appear to be relatively unaffected by the field as current has no path to ground in those directions.

2.4 Equipment

2.4.1 Universal Laser Systems X2-660

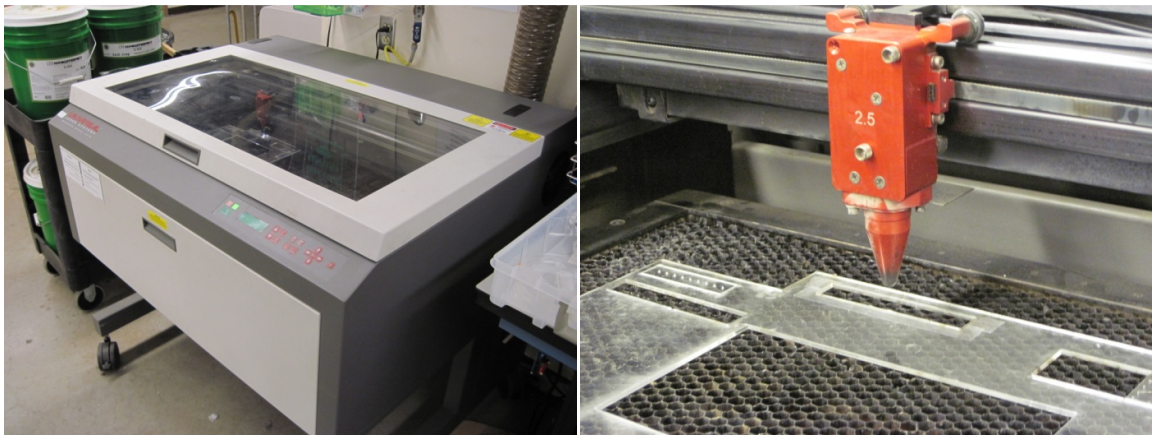

Figure 32:(Left) Laser System as it sits in the machine shop. (Right) Laser head within the system hovering over a cut piece of PMMA

The laser used in this project was a part of the Universal Laser Systems X2-660. The machine is located in the Bonderson building within the Mustang 60 Machine Shop on the Cal Poly campus. The laser cell used by this machine is 120 watts and operates at a radio frequency of 40MHz within the plasma tube [22]. According to the laser's operations manual, it emits photons at a frequency of 10.6 microns, and has a beam diameter of .005 inches. The laser system features settings that allow one to control its power, speed, and pulse density, or pulses per inch (PPI). PPI is a consequence of the system not being continually on; in other words, the laser turns on and off very quickly creating pulses. This laser has a maximum resolution of 1000 PPI, which means the distance between pulses is around 25 microns.

2.4.2 Micro-Osmette

Figure 33: Micro-Osmette was used to test run samples for their conductivity.

The Micro-Osmette is a machine that is designed to measure the osmolality of solutions and is located in the St. Jude lab in the Advanced Technologies Lab on the Cal Poly campus. The osmolality refers to the number of osmoles of solute particle per kilogram of solvent. An osmole is similar to a mole, except that it compensates for disassociation of compounds in solvent. Salt, or NaCl, for example is known to disassociate into sodium and chloride ions and therefore results in solution that is 2 osmoles per mole of salt. The Micro-Osmette works by measuring one of four colligative properties (properties that are based upon the number of molecules in a solution) which are all directly proportional to each other. These properties, osmotic pressure, vapor pressure, boiling point, and freezing point, can be used individually to find any other one. [38]

The Micro-Osmette finds the osmolality of a solution by measuring the decrease in temperature that is required to freeze a sample as compared to water. The addition of solutes will depress the freezing point of water which will then be related to osmolality as the amount of depression is proportional to the amount of solute. In this project the osmolality could further be used to determine the conductivity since the amount of ions added to the sample was directly proportional to the ionic strength and thus the conductivity. This method was used once it was discovered that the on-chip electrodes were an ineffective means to measure the conductivity.

2.4.3 LabSmith HVS448 High Voltage Sequencer (Model 3000)

Figure 34: Lab Smith voltage generator used to sink and source current over four different channels

Also located in the St. Jude lab, the voltage sequencer is a tool that can be used to create voltage or current across eight different channels of up to 3 kV. The equipment used in conjunction with its included software package can be used to create various waveforms in AC and DC as well as sequences of different waveforms that can be automatically programmed to run. In this project, the voltage sequencer was used to create DC voltages and

DC square waves within up to four channels. These waveforms created the electric fields that were used to drive ions out of the sample and into the waste channels.

2.4.4 Harvard Apparatus 11 plus Syringe Pump

Figure 35: Harvard Apparatus Syringe Pumps are capable of accurate dispersing or drawing small amounts of fluid over great lengths of time

Located within the St. Jude lab, several syringe pumps were used continuously in this project to dispense sample or buffer fluid into the chip. One syringe pump was hooked up to each of the inlets which allowed for individual control of the flow rate in each of the channels within the chip. The syringe pump is capable of delivering fluid over a wide range of flow rates with a wide variety of syringes. This particular project used flow rates that were anywhere between 1 to 9 milliliters per hour and used 10 milliliter syringes from Becton-Dickinson (BD).

2.5 Chip Testing / Experimental Setup

After assembly, chips were inspected visually and were checked for any sealing issues or clogging issues using food coloring and water injected into each of the inlets. If the channels appeared to function properly, the chip was flushed with distilled water, the electrodes were connected, and the inlets were connected to 10ml BD syringes. The experimental apparatus for this project consisted of three syringe pumps, the voltage sequencer, a computer, and several small beakers to catch fluid from the outlets. The setup, as it was constructed in the St. Jude Medical Lab in the Advanced Technologies Laboratory, can be seen in the figure below.

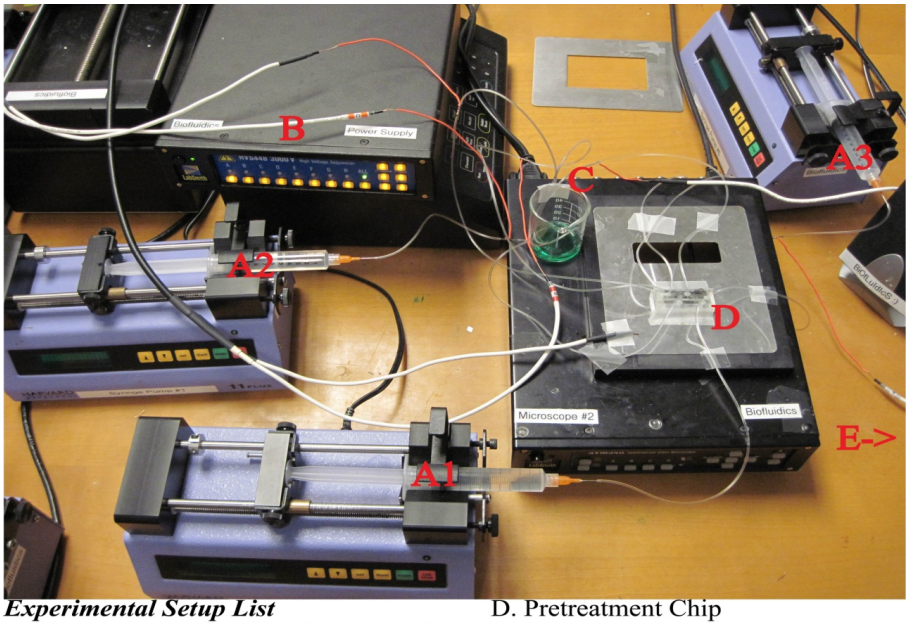

Experimental Setup List

A.Syringe Pump (Harvard Apparatus)
- A1.Sample Inlet Syringe (BD)
- A2.Electrode (+) Inlet Syringe (BD)
- A3.Electrode (-) Inlet Syringe (BD)

B. Voltage Sequencer (Labsmith)
C. Beaker
D. Pretreatment Chip
E. Computer to control 'B'

Figure 36: Experimental setup during pretreatment process. (The video microscope shown under the pretreatment chip ended up not being used)

The syringes were placed in their respective syringe pump and the electrodes were connected to the voltage sequencer. The copper electrode wire slides into the end of the high voltage

cables easily and no clip is needed. Up to four different electrode channels were used for testing. Generally, one channel would be used to source current in one of the electrode channels and another would be used to sink current in the other electrode channel. The remaining sequencer channels were used to sink or source current in other locations, such the device's sample channel. For the designed experiment, the sample syringe was filled with a saline solution with a conductivity of 1,443 mS/m to best represent blood plasma [6] while the electrode channels were filled with distilled water which had a conductivity of approximately 500 µS/cm. The flowrates were set at 8.00 ml/hr for both of the electrode channels while the flowrate for the sample channel was varied between 1, 4 and 8 ml/hr. The current was set at 0, 50, 100 and 800 microamps sinking/sourcing in each of the electrode channels such that the two channels created a current differential that is twice the level listed. For example, experiments run at the 50 microamps level would have one electrode channel sinking 50 microamps while the other channel sourced 50 microamps for a total current differential of 100 microamps.

2.5.1 Electrolysis Bubbling Problems

While this design anticipated bubbling at the electrodes as a result of the large amount of current that would be run through the sample, the bubbling still caused an unforeseen problem. The large amounts of current run through the water and salt are sufficient to allow for the disassociation of water into hydrogen and hydroxide such that hydrogen and oxygen gas can form at the electrodes. While these bubbles can be catastrophic in most microfluidic devices, it was thought that since any bubbles produced in this device would be separated from the sample by the filter, their effects would be minimal. However, as gas was formed at

the electrodes, the resistance in the chip grew as a result of the gas essentially forming a capacitive element. The current no longer had a path from one electrode to the other that did not require crossing a gas bubble. Thus the charge built up on both sides of the gas until the voltage was sufficient that the current actually arced across the gas bubble. As can be imagined, this arcing caused significant damage to the chip and the Tygon® tubing (see figure below), as well as significantly altering the electric field and flow rates within the chip. The creation of gas altered the pressures in that respective channel and, thus, the flow rate, while the disturbances in the current's flow altered the electric field.

Figure 37: Burned Tygon® tubing as a result of the arcing of current across gas created within the chip

To attempt to remedy this situation, the device assembly process was modified to include a 40 gauge copper wire that was run throughout both electrode channels. This wire was run through the channels during the initial stages of assembly and was built around such that a wire now ran from the old electrode interface with the fluid, down through the channel, and to the electrode interface in the outlet (sees figures below). This wire made the electrodes in the electrode channels continuous. This allowed current to continue to flow through the channel in the presence of gas by providing the current with a low resistance path. While this solved this problem, it introduces another in the form of corrosion. Copper is much less

resistant to corrosion and could visibly be seen corroding. Both of these effects on the experiment will be discussed further in the discussion section.

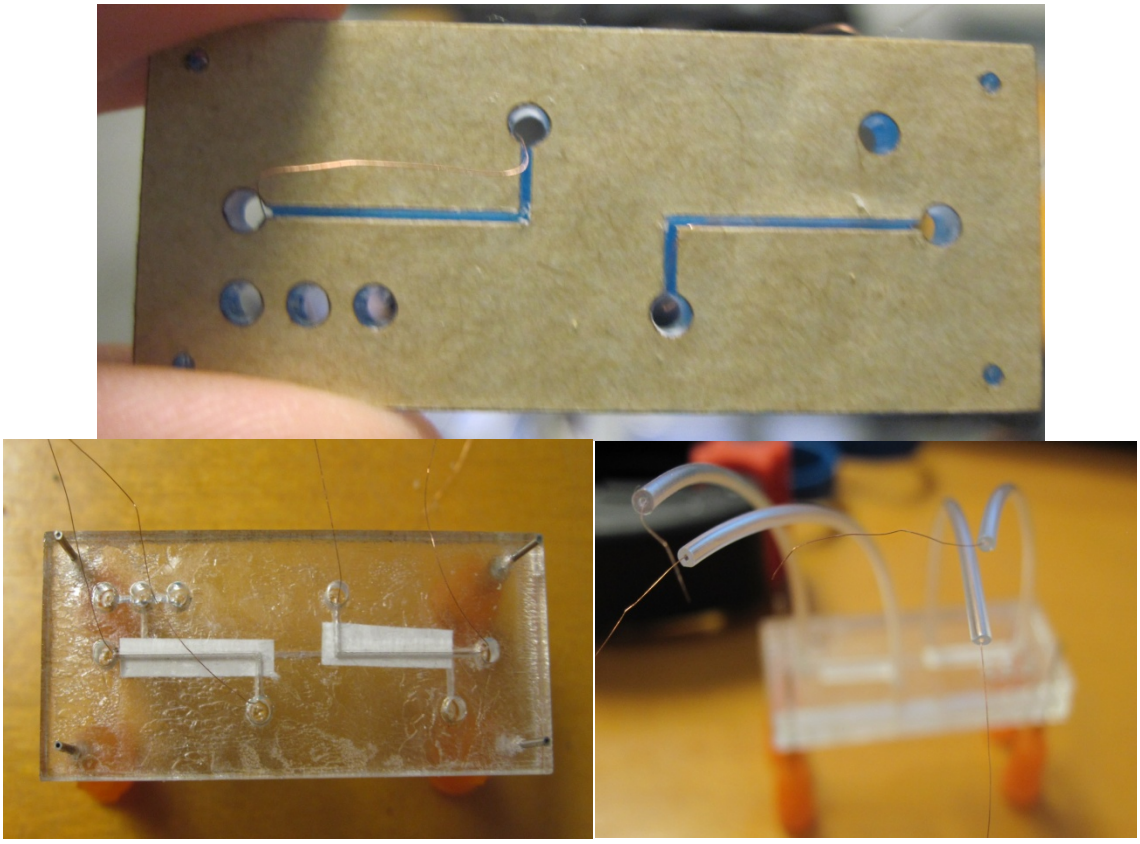

Figure 38: 40 Gauge copper wire is threaded through the electrode channels to allow current to flow in the presence of gases

III Results

3.1 Calibration Results

The following data was collected to ensure that the Micro-Osmometer could be used to measure changes in the conductivity of a solution. Several solutions were created by mixing varying amounts of reagent grade sodium chloride and distilled water, which yielded an array of solutions at different conductivities.

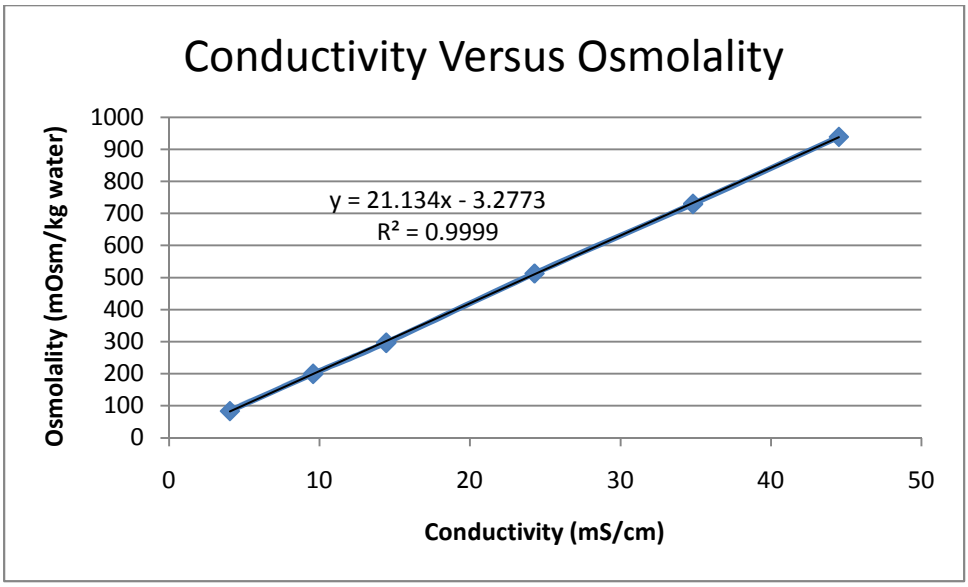

Figure 39: The conductivity of solutions were found to be linearly related to the osmolarities measured by the Micro-Osmette

These solutions then had their osmolality per kilogram water measured using the Micro-Osmometer. The graph demonstrates that there is a linear relationship between the solution's conductivity and its osmolality. The equation shown can be used to determine the conductivity of any salt water solution based upon is osmolality.

$$Conductivity = \frac{Osmolality + 3.2773}{21.134}$$

This equation was used to convert all of the osmolality readings from the data presented in the following sections into conductivities.

3.2 Initial Observations

3.2.1 Electric Field Effects on Solutions of Different Ionic Strength

This data was collected to examine the effect of the electric field on samples of different conductivities. The electrode channels were run with 1,443 mS/m saline solution while the sample channel solution was varied. All channels were run at a flow rate of 8.00 ml/hr. The positive and negative electrode channels were held at +200V and -200V, respectively. On-chip electrodes to measure the voltage were placed at the inlet and the outlet of the sample channel and the difference between the two readings was calculated. This relative measurement negated the effects of the electric field created on the chip to remove ions, as both electrodes were influenced by the field. Therefore, when the difference between them was examined, rather than their raw magnitudes, the field's effect was removed.

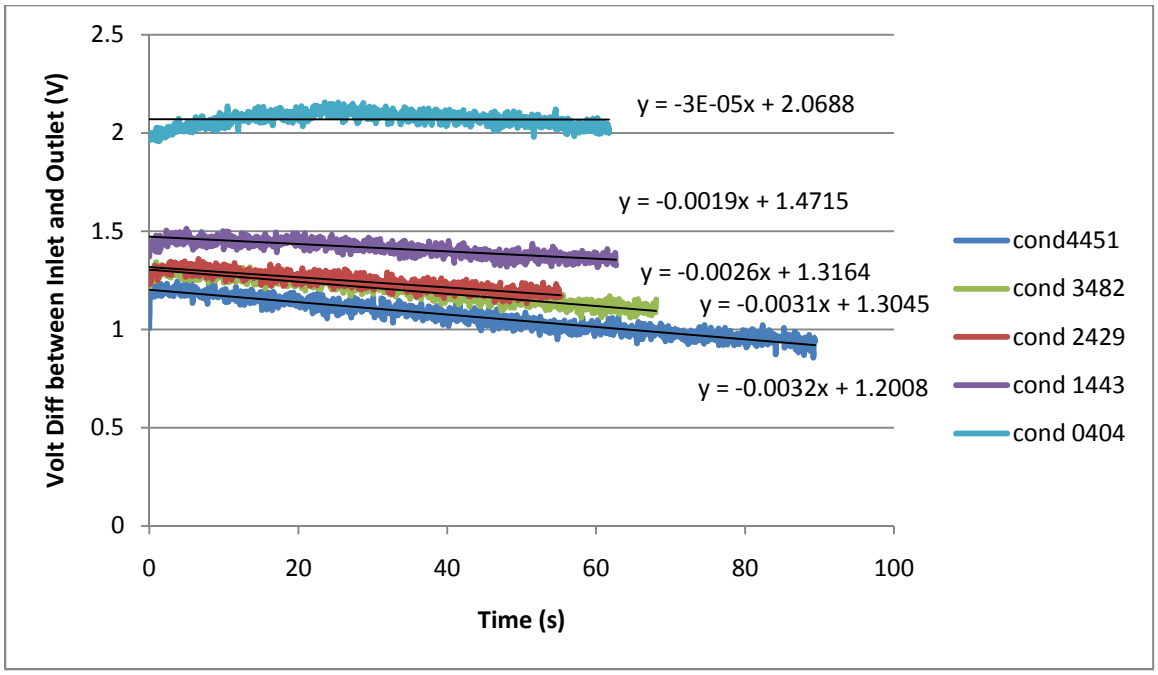

Figure 40: Voltage differences between inlet and outlet over time using 200V DC

From this data set several trends presented themselves. The first of these to note is that, as the conductivity increases, the difference in voltage lowers. The second is that all of the voltage differences lower over time. The third is that the higher conductivity samples have their voltage difference lower quicker than low conductivity samples. The last observation is that there is a significant difference in the voltage produced by the sample that had a lower conductivity than the electrode channel's fluid.

3.2.2 Sample Channel Voltage Changes Over Time

In this experiment, we wished to observe how the voltage measured in the sample channel outlet changed over time with the injection of a bolus of sample. The electrode channels were supplied with distilled water (approx. 500 µS/cm) at 8.00 ml/hr. The sample channel was supplied with 1,443 mS/cm saline at 1.00 ml/hr, when engaged. The electrodes were

sourced/sunk at ±800V. The size of the bolus was approximately 2.22 µL after running the syringe pump for 13 seconds.

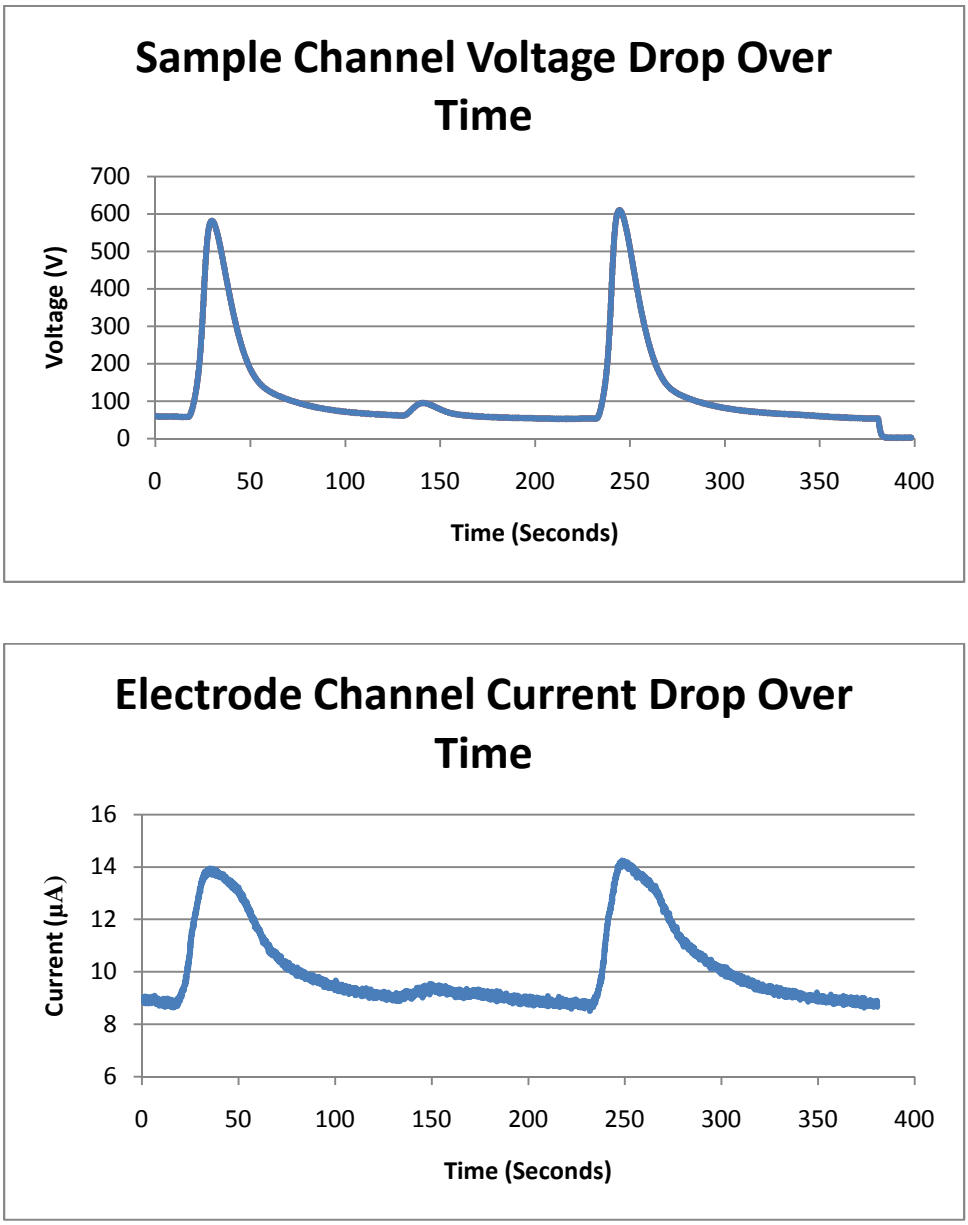

Figure 41: Two cycles of voltage and current drop over time when the sample channel injects a bolus

The voltage and current can be seen rising and dropping as the ions are introduced in the sample channel bolus. When the sample channel flow is turned back on for approximately 13

seconds, the voltage quickly rises again. The voltage is an indicator of the conductivity of the sample channel fluid and thus the ionic concentration. The combination of voltage and current describe the resistance which is inversely related to the conductivity.

3.2.3 Other Observations

Before beginning a designed experiment, many factors were experimented with to attempt to find the conditions at which the ion removal was optimal. This data is offered to 1) demonstrate that under the right conditions a sample can be pretreated to 80% of its original conductivity using this approach and 2) to merely provide additional data that was gathered that may be of interest should any future work be done on this project.

Table 6: Selected observations for DC pulse testing

Pulse DC Waveform Data			
Voltage Upstream Electrode	**Voltage downstream Electrode**	**MiliOsmolality / Kilogram H20**	**Observations**
1000	0	330	Sample Channel flow rate 8.00 ml/hr
-1000	0	305	
0	0	299	
600	-600	304	Arcing
600	-600	294	Only Sample Channel Running
-300	300	285	New day of testing
400	-400	279	Sample Channel flow rate to 4.00 ml/hr
400	-400	232	Flow stopped
400	-400	280	E channel supplied with DI water, not 1,443 mS/cm
1200	-1200	276	No bubbles in E channels with DI
1500	-1500	249	New chip with gap in filter
1500	-1500	252	
1500	-1500	261	

Table 7: Selected observations from DC testing with various parameters

DC Waveform Data			
Voltage Upstream Electrode	**Voltage downstream Electrode**	**miliOsmolality / Kilogram H20**	**Observations**
1500	-1500	237	Gap in filter and last setting from DC pulse
1500	-1500	252	
1500	-1500	255	
1500	-1500	124	Sample channel flow rate to 1.00 ml/hr
1500	-1500	127	
1500	-1500	126	
0	0	135	Considerable amount of DI entering sample channel
1500	-1500	141	Electrode channel flow rate to 4.00 ml/hr
1500	-1500	162	
1500	-1500	161	
3000	0	137	Electrode channel flow rate to 8.00 ml/hr
3000	0	152	
3000	0	148	
0	-3000	143	
0	-3000	146	
0	-3000	143	
1500	-1500	60	Side by Side chip with large sample channel
1500	-1500	61	
1500	-1500	61	
0	0	74	
800	-800	181	Bolus testing
800	-800	113	longer residence time than above sample
800	-800	83	longer residence time than above sample

3.3 Design of Experiment

To best determine the statistical effects of flow rate and current intensity on the removal of ions from the sample channel, an experiment was designed to test these factors on several levels. The experiment was run as specified in section 2.5 and the results are presented below:

Table 8: Raw data collected in a randomized design of experiment to discover the effect of sample flow rate and current intensity on conductivity

Sample Number	Sample Flow Rate (ml/hr)	Current Strength (μA)	Osmolality (mOsm/kg H_20)	Conductivity (mS/cm)
1	1.00	100	211	10.13898457
2	4.00	50	265	12.69410902
3	8.00	0	280	13.40386581
4	1.00	0	214	10.28093593
5	4.00	50	278	13.30923157
6	8.00	50	282	13.49850005
7	4.00	0	281	13.45118293
8	8.00	0	287	13.73508564
9	4.00	800	235	11.27459544
10	4.00	800	230	11.03800984
11	8.00	800	284	13.59313429
12	4.00	0	282	13.49850005
13	1.00	50	252	12.07898647
14	8.00	100	281	13.45118293
15	4.00	800	277	13.26191445
16	1.00	100	241	11.55849815
17	4.00	100	287	13.73508564
18	4.00	0	296	14.16093972
19	8.00	800	280	13.40386581
20	4.00	100	280	13.40386581
21	4.00	100	272	13.02532885
22	8.00	800	282	13.49850005
23	1.00	800	247	11.84240087
24	8.00	50	300	14.3502082
25	4.00	50	300	14.3502082
26	1.00	50	281	13.45118293
27	1.00	800	246	11.79508375
28	1.00	0	273	13.07264597
29	8.00	0	294	14.06630548
30	1.00	800	237	11.36922968
31	8.00	50	296	14.16093972
32	1.00	50	244	11.70044951
33	1.00	0	254	12.17362071
34	1.00	100	274	13.11996309
35	8.00	100	286	13.68776852
36	8.00	100	291	13.92435412
			Chip Replaced	

The table presents the data in the order in which the samples were taken. The samples' number was randomized to minimize the effects of corrosion and any other factors that would change with time. Once the data was collected, the data was analyzed with minitab. The data was fit with a general linear model with two factors of flow rate and current intensity, as well as the interaction between them. The conductivity was used as the response variable. The model generated the following results:

General Linear Model: Conductivity versus Sample Flow , Current

```
Factor                    Type   Levels  Values
Sample Flow Rate (ml/hr)  fixed       3  1, 4, 8
Current Strength (µA)     fixed       4  0, 50, 100, 800
```

Analysis of Variance for Conductivity (mS/cm), using Adjusted SS for Tests

Source	DF	Seq SS	Adj SS	Adj MS	F	P
Sample Flow Rate (ml/hr)	2	21.2101	21.2101	10.6050	15.87	**0.000**
Current Strength (µA)	3	4.4972	4.4972	1.4991	2.24	**0.109**
Sample Flow Rate (ml/hr)* Current Strength (µA)	6	3.4378	3.4378	0.5730	0.86	**0.540**
Error	24	16.0425	16.0425	0.6684		
Total	35	45.1877				

S = 0.817581 R-Sq = 64.50% R-Sq(adj) = 48.23%

Unusual Observations for Conductivity (mS/cm)

Obs	Conductivity (mS/cm)	Fit	SE Fit	Residual	St Resid
1	10.1390	11.6058	0.4720	-1.4668	-2.20 R
4	10.2809	11.8424	0.4720	-1.5615	-2.34 R
15	13.2619	11.8582	0.4720	1.4037	2.10 R
34	13.1200	11.6058	0.4720	1.5141	2.27 R

R denotes an observation with a large standardized residual.

This output, while perhaps initially daunting, presents far more information than most would be interested in. However, the information is provided for those that have a statistical

background and may find the additional information interesting or useful. Of particular interest to all are the P values, which were bolded to make them easier to find. From this analysis we can state that there is a statistically significant difference in conductivity between samples run at different flow rates. Additionally, we can say with 89% confidence that there is a difference in conductivity between samples run at different current intensities. This is a result that is generally considered not statistically significant. Furthermore, it should be noted that four observations were found to have an abnormally large standardized residual, which are commonly called outliers. The final conclusion from this data is that there is no difference in the conductivity of samples due to the interaction of both current intensity and flow rate. From this data additional graphs were produced to verify that the assumptions used in developing the model were valid.

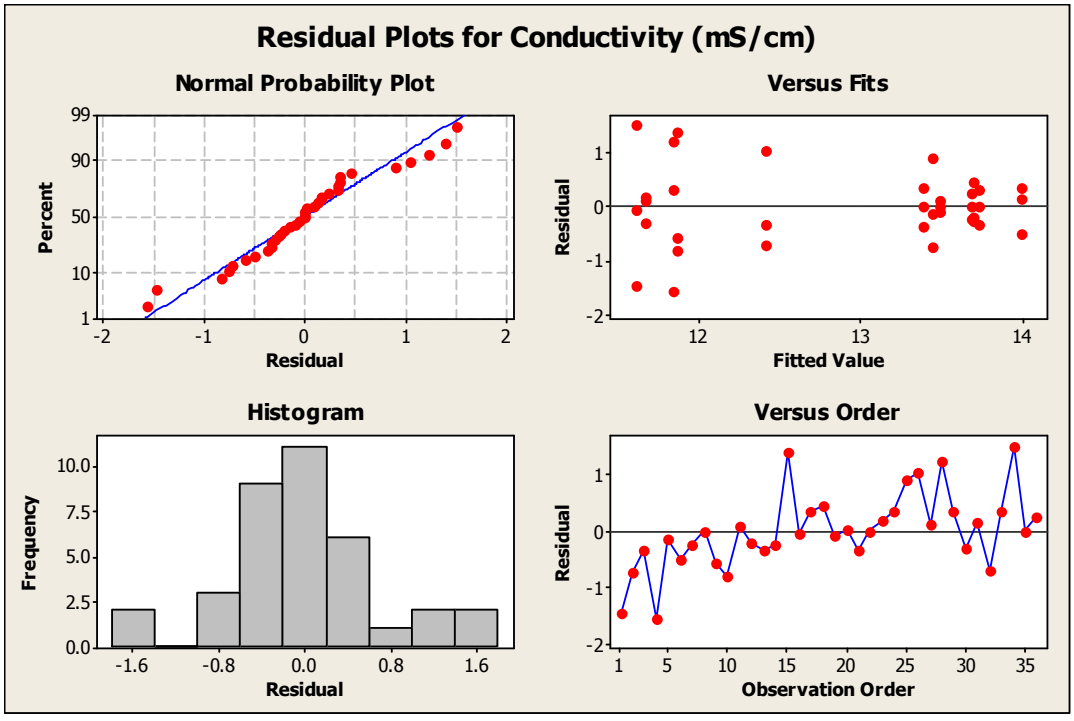

Figure 42: Four plots that are used to verify that the assumption about the conductivity data used to generate the model are valid

These plots demonstrate that assumptions made using a general linear model for this data are valid. The normal probability plot checks that the data is, in fact, normal. The points on the extreme ends are those that were listed as having abnormally high standardized residuals. This means that they were significantly different than other similar data points. A good way to think about residuals is to think of them as being similar to error, except that they also specify if the error was above or below what was expected. Given that two of these observations (1 and 15) occurred as the first run of a chip, the model was rerun to include the chip number as a covariate. This statistically removes the effect of changing the chip on the results and produces the following analysis:

General Linear Model: Conductivity versus Sample Flow , Current Stre

Factor	Type	Levels	Values
Sample Flow Rate (ml/hr)	fixed	3	1, 4, 8
Current Strength (µA)	fixed	4	0, 50, 100, 800

Analysis of Variance for Conductivity (mS/cm), using Adjusted SS for Tests

Source	DF	Seq SS	Adj SS	Adj MS	F	P
Chip Number	1	3.1793	7.5563	7.5563	20.48	**0.000**
Sample Flow Rate (ml/hr)	2	24.8387	25.4234	12.7117	34.45	**0.000**
Current Strength (µA)	3	6.5869	6.5148	2.1716	5.89	**0.004**
Sample Flow Rate (ml/hr)* Current Strength (µA)	6	2.0966	2.0966	0.3494	0.95	**0.481**
Error	23	8.4862	8.4862	0.3690		
Total	35	45.1877				

S = 0.607426 R-Sq = 81.22% R-Sq(adj) = 71.42%

Term	Coef	SE Coef	T	P
Constant	11.1892	0.3923	28.52	0.000
Chip Number	1.0646	0.2353	4.53	0.000

Unusual Observations for Conductivity (mS/cm)

Obs	Conductivity (mS/cm)	Fit	SE Fit	Residual	St Resid
32	11.7004	12.7651	0.3594	-1.0646	-2.17 R

```
34       13.1200  11.9607  0.3594    1.1593      2.37 R
```

As can be seen from the p values in this model, the current strength is now shown as making a statistically significant difference on the conductivity of the sample. While the p value of the interaction changed as well, the result remains the same as before. The plots to check assumptions were once again generated for this model.

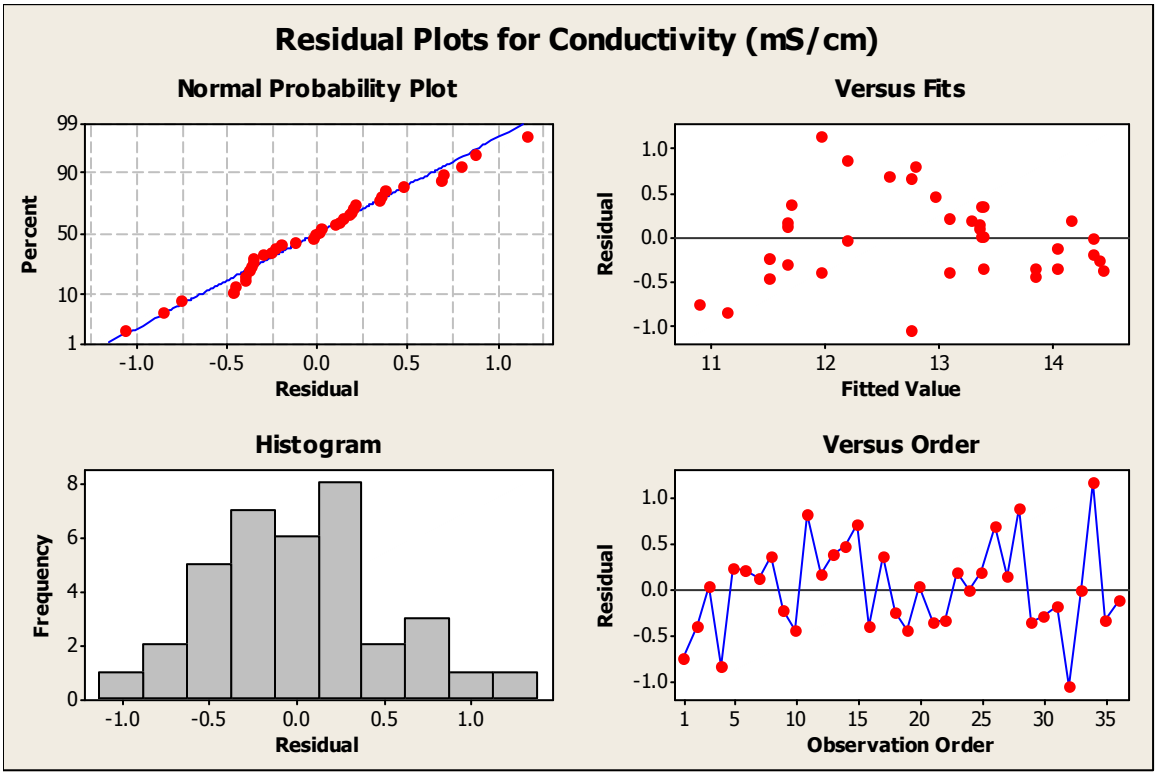

Figure 43: Second set of plot use to check assumptions of second statistical model

The plots produced by this model demonstrate the model fits the data much better. The "versus fit" and "histogram" plot visualize the distribution of the residuals which appear to be well distributed in the histogram. However, the "versus fit" plot appears to have a slight bias in that higher conductivity measurements had less error than low conductivity measurements. The "versus order" plot visualizes how error changed over time. The trend in the first model appears to have disappeared now that we have accounted for the chip change.

Two additional plots were generated to see how the factors related to the residuals. These plots illustrate if there was a large amount of consistency in the result produced at a particular level of a factor or if there is a considerable amount of variation from observation to observation.

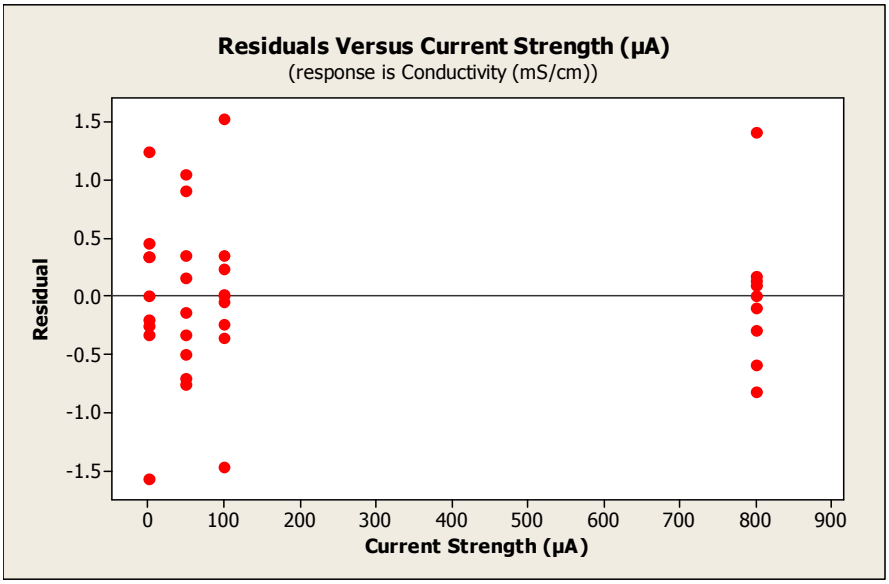

Figure 44: Residuals at each level of current strength. The residuals appear to be fairly even across each of the levels on current strength.

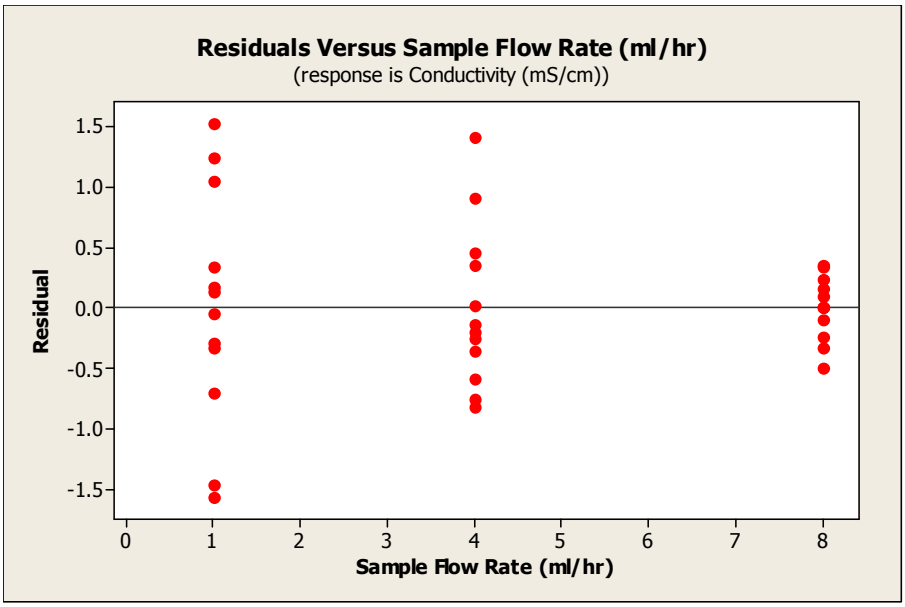

Figure 45: Residuals at each level of sample flow rate. The residuals appear to less as flow rate increases.

The only point of note in these graphs is the difference in variance between the different levels of flow rate. Lower flow rates produced values that were more varied than higher flow rates.

IV Conclusions / Discussion

4.1 Initial Observations Discussion

4.1.1 Electric Field Effects on Solutions of Different Ionic Strengths

The data presented in this section of the results was a preliminary test that was aimed at characterizing how the chip would handle pretreatment of solutions of different ionic strength. As mentioned prior, several trends appeared in the data. The first of these was that the difference in voltage between the inlet and outlet of the sample channel was smallest in high conductivity samples. We believe that since ions have such high electrophoretic mobility, the voltage difference was primarily created by a lack of ions to carry current, not a time lapse due to their mobility. The lower ionic strength sample experienced a higher voltage difference as there were insufficient ions in solution to carry the charge. Since this measurement was a relative measurement, the voltage difference is a result of the outflow voltage being higher than the inlet. This results from an increase in resistance and decrease in current flow. A higher voltage difference, created with the low conductivity sample, indicates that the device altered the ionic strength more. It appears that when less ions were provided to the system, the system was more efficient are removing ions.

Figure 46: Syringes prepared with saline solutions of varying ionic strength

The second observation was that all of the voltage differences lower over time. This could simply be the result of the chip moving towards an equilibrium point since the sample channel's would-be flow was run for some time before turning on the electric field. Since the third observation was that that the higher conductivity samples appear to have their voltage differences lowering faster than the lower conductivity samples, the second observation is likely also related to ionic strength. Looking closer at the data, it was noted that both the inlet and outlet voltage changed over time with the inlet increasing more. Since the current remained fairly stable this means that the resistance of the outlet and particularly the inlet increased over time. All of which indicates that there is a stabilization period in the chip that lasts longer than sixty seconds. Since the lowest conductivity sample did not seem to follow this trend, it could be concluded that the more conductive samples take more time to reach a point of stable voltage and that the low conductivity sample already had. This data indicates that the chip becomes less effective over time as the extra ions introduced into the chip begin to build up. Unfortunately, this also means that any data taken without running the chip for a significant amount of time is likely to be vary based upon the time that it was run.

4.1.2 Sample Channel Voltage Changes Over Time

This experiment was designed to look more closely at the time response of voltage within the sample channel. Rather than probe the whole length of the channel which provides somewhat of an average of the whole sample, we choose to look at the outlet of the sample channel specifically. As demonstrated in the results section, a nice curve was produced that characterized how the voltage in the sample outlet changed over time. As the bolus was introduced, the excess of ions caused a dramatic increase in the voltage between the electrodes at the outlet. Looking at the electrode current confirms that ions lowered the resistance in the electrode channels as voltage was held constant. It would appear that after around 50 seconds the ion excess has been removed by the fluid flow.

We would expect the resistance to drop in the sample channel, and thus the voltage, as ions from the bolus reach the outlet. However, the voltage increased, which would indicate that the current dramatically increased. Unfortunately, this explanation does not seem logical given that the current never exceeded several hundred microamps in this project. A more likely explanation is that not all of the gas between the sample channel electrodes and fluid had been removed. This would add a capacitive element that charged up when ions were introduced. Current looking for a path to ground caused ions to accumulate at the surface of the gas and the electrode, dramatically increasing the voltage. This explanation provides a rational for the exponential decay of the voltage, but makes previously assumed cycle time inaccurate. Given that the other experiments in this project would be run continuously, no further work was done to attempt to predict the time for the system to return to equilibrium. However, this experiment did serve to illustrate how charge could be built up on-chip in any number of places from experiment to experiment.

4.1.3 Other Observations

This additional data is given as a point of reference for future researchers. The first table outlines the DC pulse testing, which was performed due to the success that Tim Abram's project had with this waveform. It was thought that if a simple DC waveform was not successful in removing ions, that perhaps pulsating the voltage would create the desired effect. However, after numerous samples were run with different parameters, no notable difference was observed and the waveform only served to complicate matters. Thus, a simple DC waveform was used for the designed experiment. From these experiments it was noted that the flow rate seemed to have a substantial effect on the conductivity and that having lower conductivity solutions in the electrode channels appeared to also reduce the conductivity.

The second data table presents the data gathered from experiments using a simple DC waveform. Several different parameters were played with in this data set. The first of these was to create a gap in the filter membrane, which disrupted a continuous layer of filter from one electrode channel to the other. This was motivated by the idea that the filter might be sufficiently thick to allow the electric field to largely pass through it, rather than the sample channel. No statistics were performed, but the difference appeared to be insignificant. The simple DC testing also led to the discovery that the placement of the outlet tubes influenced the amount of dilution that occurred in the chip. Much of the data on this table reflects the outlet tubes being loosely placed into beakers that at times were full of fluid from previous runs. It was discovered that the hydrostatic pressure was enough to increase the resistance of submerged outlets and drive fluid towards the other exits. When the waste outlets were submerged, electrode channel fluid of less ionic strength was forced into the sample channel,

which caused a reduction in the measured conductivity. The opposite occurred if the sample channel outlet was submerged rather than the waste outlets, which slowed sample collection and likely increased measured conductivity.

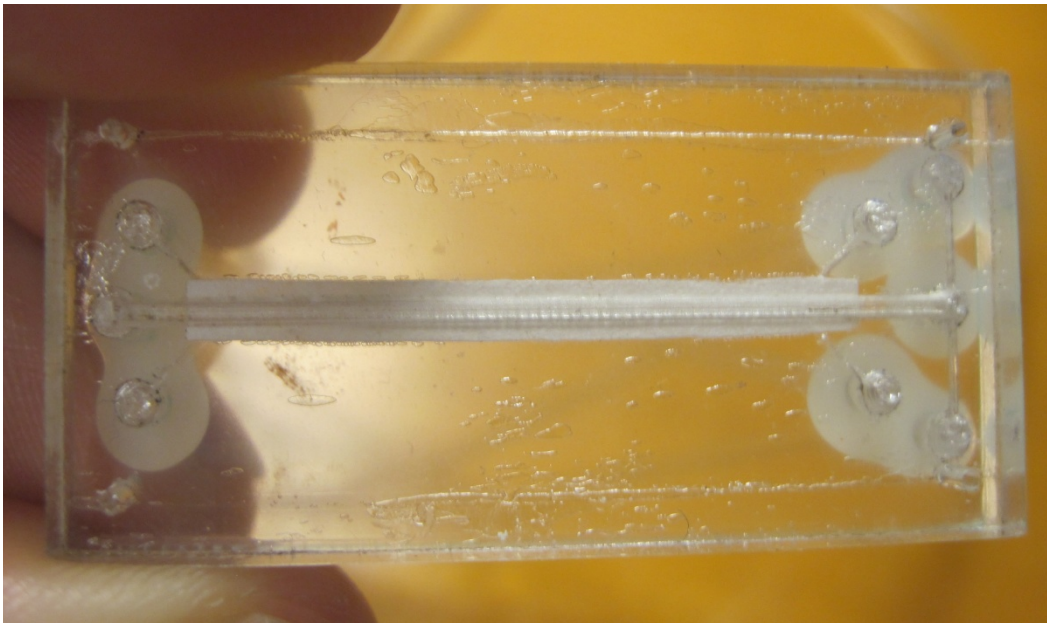

Figure 47: The widened sample channel of the redesigned side by side electrode channel chip

The data from testing the other chip design is included in this table as it was tested using simple DC waveforms. The chip demonstrated the lowest conductivity results that were collected during this project. However, for the same fluid resistance related issues described above, these results were primarily attributed to dilution rather than the electric field. The wider sample channel aimed at increasing the retention time, also greatly reduced the resistance in the sample channel relative to the electrode channels. A significant amount of fluid crossed from the electrode channels to the sample channel to follow the path of least resistance. However, while this design functioned primarily through dilution, the reduction in conductivity was in the target range. With only a few tests the chip was found reducing the conductivity of the sample by approximately 80 percent. Despite this result, the difficulty in

knowing the degree to which each factor lowered the conductivity discouraged the use of this design.

The last data points on the table refer to data that was taken during the previous experiment involving the injection of a bolus of sample. These observations reflect that as residence time increased in the chip, the conductivity of the sample lowered. A principle that was observed across all of these experiments and that should be taken in consideration for any future work.

4.2 Designed Experiment Discussion

The designed experiment of this project was developed to illustrate whether flow rate of the sample channel and current intensity caused a difference in output sample conductivity. These factors were chosen because the former correlated to the amount of dilution in the previous experiments and the later could be related to the electric field created in the chip. The experiment was not designed to maximize the conductivity reduction, given that it had been discovered that the parameters required to achieve those results were found to be destructive to the chip and its interfacing. These same destructive effects motivated randomizing the sample order to minimize their effects on the data. Despite this effort, the corrosion of the copper wire occurred much quicker than expected and required a second chip to be used halfway through the testing.

The first model fit to the data did not take this into account, but provided four outliers, of which two included the first sample run on a new chip. Given the evidence in other experiments relating to the time required for a chip to stabilize electrically and the error found in these two points, another model was fit to the data. The model was fit in the same way, but included the chip number as a covariate. Both models indicated that the flow rate

caused a statistically significant difference in the conductivity of the sample. Based upon the F-statistic, it is clear that that flow rate is also the factor that explains most of the variance in the data. In other words, the flow rate is responsible for the majority of the change in the conductivity. A conclusion that indicates the importance of retention time and that dilution was more effective on this chip. The two models disagree about whether current intensity caused a statistically significant difference in the conductivity of the sample. However, in the model that suggests it is not a significant factor, this is by a narrow margin. Given this fact and that the R-squared value for the fit of a model is higher in the second model, we believe that the electric field caused a significant difference. Regardless of these two significant factors, it would appear from the analysis, that many of the effects controlling the conductivity of the sample are left unknown. These could be any number of factors, for instance the hydrostatic pressure from outflow tubes being submerged within a beaker or built up capacitive charges that we not allowed to reach equilibrium before the next experiment. Nevertheless, this experiment answered our questions about the influence of flow rate and electric fields.

4.2.1 Model Assumptions

The plots generated to validate general linear model assumptions, provide evidence that this model is a good choice for the data. These assumptions are that the data has independence, homogeneity of variance, normality of error and linearity [39]. Independence refers to an assumption that the data was drawn at random from one homogenous pool of data, rather than one that consists of subsets. Before including the chip number as a covariate, the data came from two subsets, chip one and chip two, and was not independent. Including chip

number as a covariate accounted for this and made the second model more appropriate for the data.

Homogeneity of variance refers to the notion that the data should be randomly distributed. In this case, we observed two ways in which the residuals appeared to have trends, rather than randomness. In samples where conductivity was reduced very little, there was very little variance when compared with samples that had their conductivity reduced more significantly. This result indicates that not all the factors influencing conductivity reduction were accounted for. We also observed that when the flow rate was higher, the conductivity values were more regular and stable. However, when flow rates were lower, the conductivity measurements were more erratic. These two observations imply that the other factors unaccounted for, were related to fluid flow rather than electrical factors.

The normality of error refers to the distribution of the residuals in the model. Since the data is shown as being normal in the normality plot, we did not worry about this assumption.

The linearity of the data refers to the notion that the factors need to be linearly related to the response variable. Ensuring that this assumption is met requires examining each of the factors influence on the data independently and ensuring that a transformation is not required. A transformation that significantly improved the fit of this data was not found.

While the results of checking these assumptions were not ideal, believe that this model is well suited to the data and its conclusions accurate. While the error in the model may be troubling to some, without a method to instantly observe the movement of ions in the chip, it is very difficult to know what factors were influencing the final osmolality reading. For this project, there was a black box between the inlet of the sample channel and the sample vial as

it was placed into the Micro-Osmette. Without a feasible method to visualize the movement of ions, we were left to theorize and hypothesize with only moderate success.

4.2.2 Electrolysis and Corrosion

By manufacturing the chips used in the designed experiment to include copper wire, it was hoped that problems created by the electrolytic formation of gases would be avoided. While the gas continued to be produced on the chip, the copper wire provided a solution by providing the current a conductive path across areas of gas created within the channels and tubing. However, the very fine copper wire was not corrosion resistant and was found to quickly corrode in the initial runs of the experiment. The wires seen in the figure below have corroded to the point that the anode has completely separated from itself.

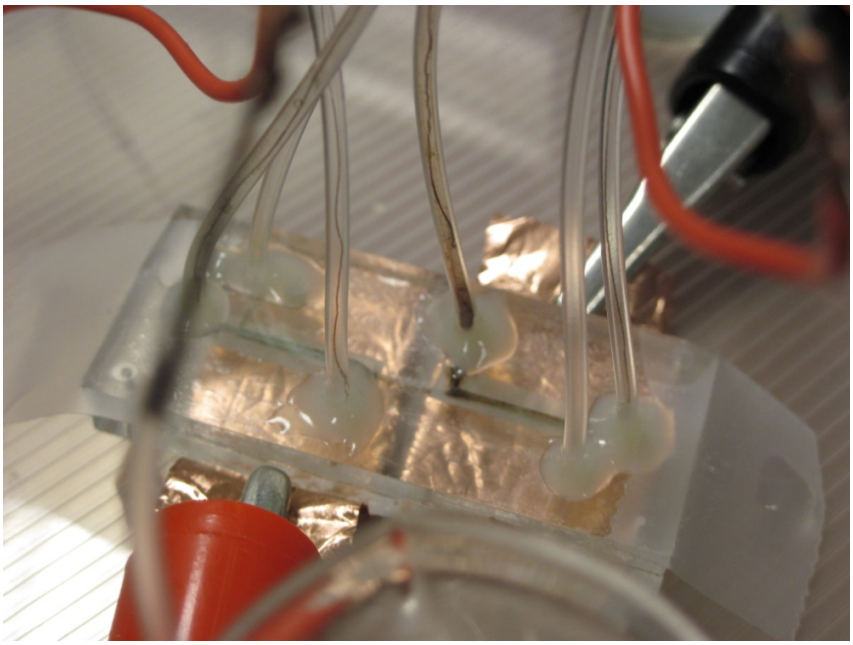

Figure 48: The copper wire anode can be seen totally detached after degrading while the electrode channel on the left side shows the cathode with a teal tint from the copper oxide production. This photo also shows copper tape used to attempt to create a capacitive force which was later abandoned.

The cathode appeared to create a copper oxide which created a layer of electrical insulation on the wire. This layer impeded the current and dramatically increased the voltage required to reach the specified current. The anode, alternatively, appeared to dissolve copper ions into the electrode channel and eventually caused the wire to burn all the way through. Unfortunately, this required replacing the chip midway through the experiment and the introduction of another factor into the experiment. As well, the effects of both electrolysis and corrosion likely had an unmeasured effect on the efficiency of ion removal on-chip. Using the versus order graph from the first model, the effect of corrosion on the efficiency of the chips can be seen over time. The general trend of increasing conductivity with each successive run suggests that the electrodes were becoming less effective at removing ions over time. A solution to these problems may exist in a different electrode design or in different material selection. However, while initial experiments would have to be stopped completely if bubbles were trapped in the right locations, the degradation rate of the copper wire, is at an unacceptable level. Even if this chip was a single use device, like when used in its real world application, the corrosion may lead to undesired contaminants in the sample. These two phenomena created a situation which overcoming could be the source of a whole separate thesis.

4.3 Future Work

4.3.1 Electrodialysis

One of the methods used in industry to treat solutions for conductivity, in the specific form of ions, is electrodialysis. Electrodialysis is used in several applications, from water treatment schemes to dialysis machines used for renal failure. In both cases, electrodialysis is used to

remove ions and other charged species from solutions. Therefore, the design of these machines has the potential to be used in a microfluidic application.

An electrodialysis machine removes ions through the use of ion selective membranes, which permit the flow of only one polarity of charged species. Using the simplistic example of a saline solution comprised of NaCl, the electrodialysis machine would feature several parallel channels with ion selective membranes between them. One interface with a sample channel would be a Na selective membrane and only allow sodium to pass through it and the other interface would be a Cl selective membrane (see figure below).

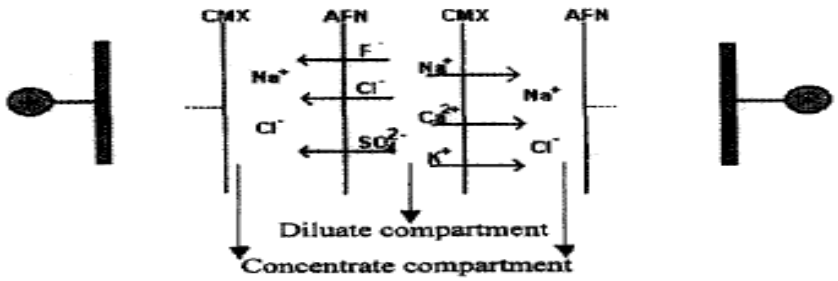

Figure 49: Electrodialysis system schematic. The anion permeable membrane is labeled AFN, while the cation permeable membrane is label CMX. The electrode on the left is positively charged while the electrode on the right is negatively charged [40]

The diluate compartment shown in the figure illustrates the described setup. An electric field is created perpendicular to flow to create a force on charged species in the diluate compartment. The anions are attracted to the positive pole and cross the anion permeable membrane, while the cations behave similarly but move toward the negative pole. Once across the membrane they continue to be attracted to their respective poles and do not diffuse back into the diluate compartment. The ions originally in the concentrate compartments are unable to cross into the diluate compartment because they are either attracted to pole of the channel they are already in, or are unable to cross the selective membrane. This allows for the

creation of several of these configurations to be arranged in parallel to create a ‘stack’. A stack design in an electrodialysis apparatus is shown below.

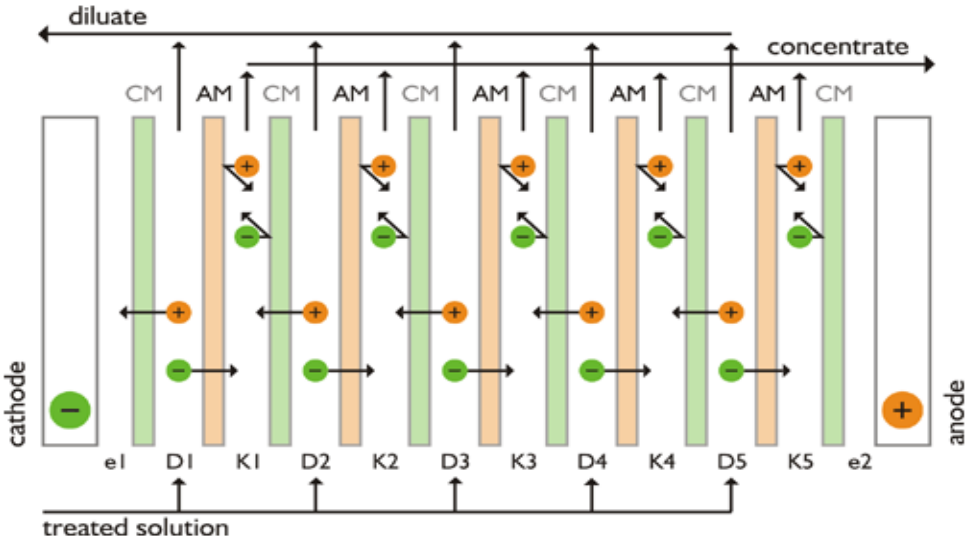

Figure 50: Several sets of selective membranes are placed in parallel to create a stack and increase the efficiency of process. CM - cation exchange membrane, D - diluate chamber, e1,e2 – electrode chambers, AM - anion exchange membrane, K - concentrate chamber [41]

Using the clamshell design developed in this project, an electrodialysis machine could be created on-chip. Using something similar to figure shown above, a micro scale electrodialysis machine could be created by alternating channels from one half of the clamshell to the other. This would allow for the selective membranes to interface with two channels while providing for the macro scale handling of the filters. The most difficult aspect of this design, would be manufacturing the chip with alternating selective membranes, however such a challenge is feasible. This design could greatly improve the magnitude of conductivity reduction possible on-chip, as many industrial systems boast of conductivity ratios of up to 20 to 1 [42].

4.3.2 Conductive Dyes

One issue of this project that caused uncertainty was the fact that ions could not be visualized. All of data collected in this project had to be done with continuous or semi-continuous flow and required taking measurements after the run of the experiment. Many of the potential factors influencing the movement of ions within the chip could not be seen as the chip was somewhat like a black box. One possible solution to this problem would be the use of conductive dyes. There are dyes on the market available called rhodamines. These dyes fluoresce and can be easily detected, while also containing regions that are polar. Adding this dye to samples run though our microfluidic device could allow for visualization of how charge species migrated within the chip. One potential drawback is that these dye molecules are considerably larger than ions, as almost any molecule will be, and their behavior may differ from ions. Yet, we believe that the size would only affect the magnitude of forces not the particles behavior. At the least, the dye would provide some idea as to how charge particles moved in the chip.

4.3.3 Design for retention time

One observation that was consistent across all of the experiments performed in this project, was that retention time significantly affected the end conductivity of the sample. Depending upon the flow rate used in these experiments, the retention time varied anywhere from 2 to 15 seconds, with 2 seconds being the time for the 8.00 ml/hr flow rate. An increase in retention allows for both more dilution to occur as well as more ion removal via the electric field. In future designs, this value could be increased by lengthening the channel. One clever method

from literature involves the use of serpentine channels [43]. These lengthen the channel without significantly increasing the size of the device.

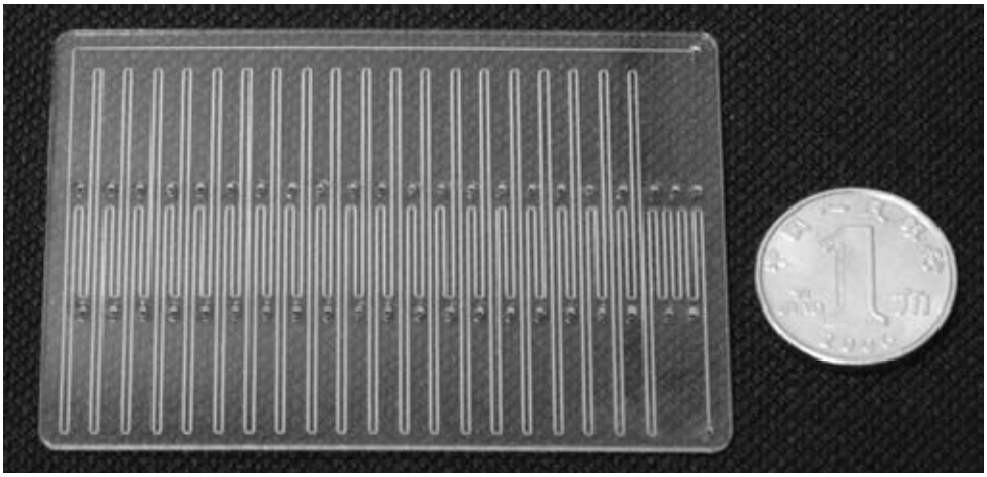

Figure 51: Serpentine design used in PMMA microfluidic device manufactured with laser ablation for PCR [43]

Since this project still requires the use of a macro scale filter, a clamshell design that incorporated this serpentine pattern into the route of the sample channel, is one potential design. Additionally, the electrode channels could also be designed in a serpentine fashion, but perpendicular to the sample channels to maximize the interface area between the two channels. Using this style design could easily increase the residence time to over a minute or more, depending on the flow rate.

4.4 Concluding Remarks

This project was successful in demonstrating the combination of dilution and electric fields in the pretreatment of solutions with physiological ionic strength. By removing ions and adding deionized water, sample solutions had their conductivity reduced in preparation for downstream separation or analysis. However, in many cases, additional sample volume from

dilution is not desirable and can lead to increased processing time for downstream processes. It was hoped that the electrical fields would have a more substantial effect on the ion removal process, but it appeared the approach was hampered by many different effects. The electrolytic formation of gases greatly disturbed the electric field on chip and caused damage if not addressed. The attempted method to address the problem introduced corrosion, which had its own negative effects. Additionally, the cross sectional profile of the cut channels and the geometries of the chip were found to be less than ideal in terms of retention time. In spite of these obstacles, and likelihood of other unknown forces, the approached proved that it causes a statistically significant change in conductivity. With redesign based upon the preliminary validation work of this project, we believe that a more efficient and effective device could be produced. One which could successfully and reliably produce samples pretreated to a desired conductivity. During this project we strove to maintain the goal of producing a chip that fits with the long term applications of this field; a goal which we believe to be successfully met. Additionally, this research group's continued emphasis on low cost production will aid in this project and other's adaptation to subsequent LOC designs. LOC's substantial potential to create POC diagnostic devices has motivated this project to its completion and will hopefully inspire more work that may one day allow for early detection and proper healthcare treatment on a global scale.

V Appendices

Appendix A - Electrophoresis Theory

A.1 Protein Ionization

In a simplistic approach, any charged species is assumed to be a uniform sphere with an equal charge density throughout [44]. This charge density is based upon both the species' inherent properties as well as the pH of the solution that contains the species. At a high pH, or basic, the side groups on molecules, such as carboxyl groups or amine groups, are deprotonated, producing a negative charge. At a more neutral pH, such as that of water, some side groups attract another proton, while others remain the same. These two effects balance each other out, which create a net neutral charge. At a low pH, or acidic, the side groups on molecules adopt even more protons and therefore produce a net positive charge [44]. Proteins, for example, are composed of amino acid chains and some of these amino acids contain polar regions, or charged side groups, and are consequently influenced by electric fields and pH. A protein's net charge is what allows for it to be uniquely separated from other proteins and their medium. Therefore, the pH of the solution containing the proteins will have a substantial impact on the charge of the proteins and how they separate.

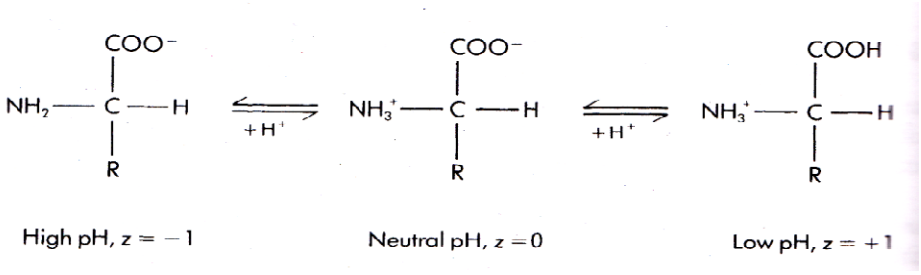

Figure 52: Ionized forms of an amino acid as a function of solution pH [44]

A.2 The Electric Double Layer

Within a state of equilibrium, the next consideration for electrophoresis is in how charges accumulate on surfaces. Most substances will acquire a surface electric charge when they are in contact with a solution containing ions, or a polar solution. As can be seen in the figure below, this surface charge will attract counter ions of the opposite charge to the surface. Particles and surfaces within a solution will thus develop what is called a “screening layer,” also known as Debye layer. If a surface has a net positive charge it will attract negative ions, or anions, which form an effective screen around the particle. The distance from the surface to the boundary where the ions become more diffuse is referred to as the Debye screening length.

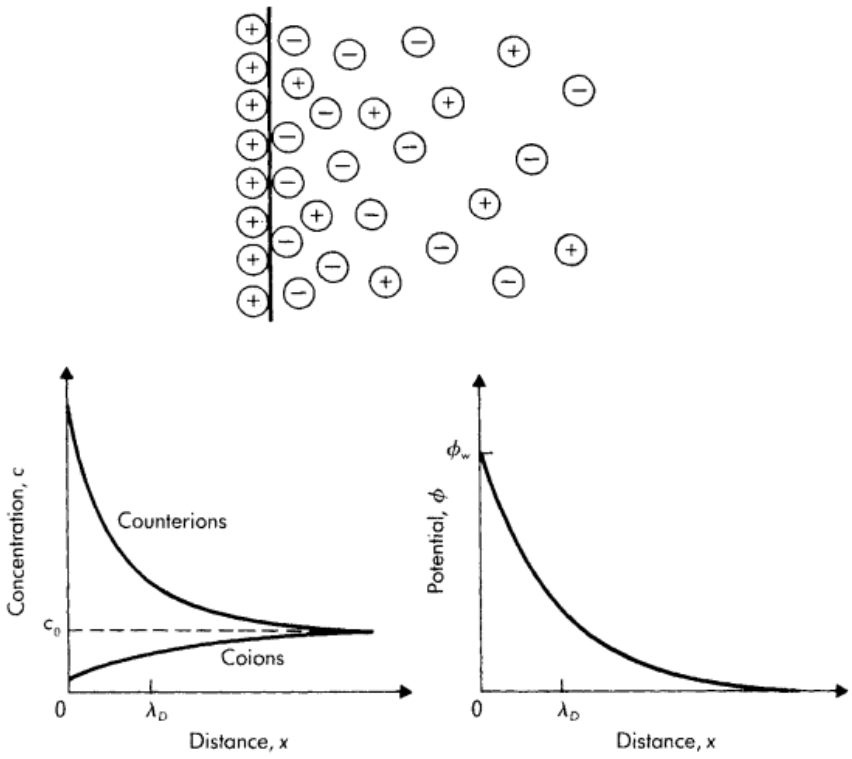

Figure 53: The electric double layer. (Top) Positive ions accumulate on the surface and attract negative counter ions. (Left) The concentration of counter ions versus co-ions as a function of the distance from the surface. Debye screening length (λ_D) is shown on x axis. (Right) Potential, or charge concentration, versus distance [44]

The Debye length is generally labeled as λ_D or k^{-1} and is expressed in nanometers. The screening layer has an impact on the movement of particles through the fluid and causes them to move slower than if it did not exist. This Debye screening length can be calculated as:

$$\lambda_D = \sqrt{\frac{\varepsilon_r \varepsilon_0 k_B T}{2e^2 N_A I}}$$

Where ε_r is the dielectric constant, ε_0 is the permittivity of free space, k_B is the Bolzmann constant, T is the temperature, e is elementary charge, N_A is Avagadro's number and I is the ionic strength of the electrolyte. In this project we used NaCl, reagent grade salt, in water at 25 °C. Thus, the equation can be simplified to:

$$\lambda_D = \frac{.304\ nm}{\sqrt{c_0}}$$

Where c_0 is the concentration in moles. To create a salt solution that was similar in conductivity to plasma (1,443 mS/m), one of solutions we used in this project, we used an approximate molarity of .4 mol / L. This results in a Debye screening length of 0.48 nm. The relationship between conductivity and concentration is a result of an increase in ions, also increasing the efficiency of screening surface charges. The calculation of the Debye length allows for further calculations concerning electrokinetics. Since ions have a radius on the order of 5 angstroms, the ratio of particle radius to Debye length, a/λ_D, is much smaller than one. This ratio will define which set of equations applies to our calculations.

A.3 Electroosmotic Flow

Electroosmotic flow is the movement of liquid relative to a stationary surface by an applied electric field [44]. Generally speaking, when most people refer to electroosmotic flow, they are referring to the effect of the charged surface of the channel on the solution flowing through it. Most materials used in microfluidics, such as the substrate, or the material that the channel is cut out of, have a negative charge [21]. Consequently, it follows that the channel walls will attract positive ions to screen this negative charge. These charges have an influence on these species that are flowing down the channel. It generally causes a net negative charge in the solution because the screening layer repels negative ions. As a result, there is a net force on the fluid to move towards the negative potential.

$$\mu_O = -\frac{\epsilon\zeta}{\eta}$$

Where μ_0 is the electroosmotic mobility, ε is the permittivity, ζ is the zeta potential of the wall, and η is the viscosity of the solution. For the purposes of calculation, PMMA, the substrate used in this process, was taken to have a zeta potential of -13 mV, according to Literature [45]. As well, the dielectric constant for the NaCl solution was taken as 73.4 from literature [46]. Finally, the viscosity of the salt solution was approximated as 0.9367 mPa*s from literature [47].

Electroosmotic mobility describes the movement of a particle relative to a fixed or stationary phase, such as a wall. For our project, the electroosmotic mobility is calculated to be -1.018 m^2/Vs. The negative value indicates that the electroosmotic force acts against the flow of the particles. Furthermore, increasing the voltage, or the electric field, will increase the strength of this force on ions in the solution.

A.4 Electrophoretic Flow

While electroosmotic flow focuses on the big picture of the flow, electrophoretic flow is concerned with each individual particle. The electrophoretic flow describes the influence of an electric field on an individual particle. The electrophoretic mobility of a particle is proportional to that particle's ionic charge and inversely proportional to frictional forces. To begin, we describe the force a particle experiences due to the electric field as:

$$F_{EF} = qE$$

In this equation describing the Columbic force F_{EF}, q is the particle surface charge and E is the strength of the electric field, most commonly given in units of V/cm. Resisting this force is the viscous force, which is due to frictional resistance in the fluid and is described as:

$$F_{FR} = 6\pi\eta r v$$

In the viscous force equation F_{FR}, η is the viscosity, r is the radius of the particle, and v is the velocity of the solution. At equilibrium we can combine these two equations into:

$$v = \frac{qE}{6\pi\eta r}$$

This equation accounts for both the 'drag' and 'pull' experience by a particle at equilibrium. The terms in this equation are the same as those described above. This equation describes the electrophoretic velocity, v, but is more commonly used to describe the electrophoretic mobility shown below:

$$\mu_p = \frac{v}{E} \text{ thus } \mu_p = \frac{q}{6\pi\eta r}$$

μ_p, the electrophoretic mobility, more accurately describes both the forces on a particle and their magnitude. For our applications, the electrophoretic mobility is huge since the radius of ions is so small and should be several orders of magnitude larger than the electroosmotic mobility. In this application the electrophoretic mobility will dominate the ions' movement.

Appendix B – Materials Selection

B.1 Manufacturability of PMMA

Interest in PMMA has grown over recent years for several reasons, despite the vast majority of microfluidics being done in PDMS. PDMS is popular because it provides the advantages

of optical clarity, ease of bonding to glass and an ability to create precise micro scale geometries from molds. However, PDMS cannot be exposed to high temperatures without losing its structure and it has been known to have a short shelf life. As well, at room temperature PDMS behaves almost like a soft rubber. This causes the material to tear from relatively low shear stresses, sag without proper support in larger microfluidic channels and require delicate handling [48]. Additionally, the soft lithography process requires expensive and harsh chemicals, as well as sensitive and expensive equipment. Thus, its applicability as a prototyping material has begun to be called into question, since research done with it will ultimately have to be performed again with a new material.

PMMA has thus been growing in attention as a possible substitute for PDMS, as it provides many of the benefits of PDMS, without some of its major drawbacks. To expound on those traits mentioned earlier, PMMA has a much higher stiffness than PDMS and, thus, is capable of producing much larger microfluidic channels without the need of supports. The material is actually less expensive than PDMS due to the lack of expensive chemicals needed in its fabrication. PMMA is more hydrophilic than PDMS, which means that it is more easily wet by most aqueous media, an advantage in most microfluidic chips. While its optical clarity is not necessarily better than PDMS, it is still clear enough to use for most testing purposes where visualization will be important. One of the largest advantages of this material is that it is very common commercially and, thus, those in the manufacturing world have been exposed to this material such that they know how to handle it, what its limits are, and ways to work around problems. This makes the transition from research to manufacturing quick and easy.

Several different approaches exist for the manufacture of microfluidic devices with PMMA. Briefly they range from such things as laser photoablation, hot embossing, x-ray lithography, plasma etching and UV patterning [49]. These are very different processes and are generally chosen based upon an intended result. Laser photoablation was chosen for this project as it is capable of producing features sufficiently small to meet the requirements of this project. It was also chosen because of the ease with which it can be performed, and the short production time. These features make this approach perfect for prototyping and far more desirable for this project, despite other processes providing better resolution. However, there are other draw backs to the approach, such as surface smoothness and surface modification issues. Considerable amounts of material are ejected, vaporized and melting during laser cutting, that result in poor surface roughness.

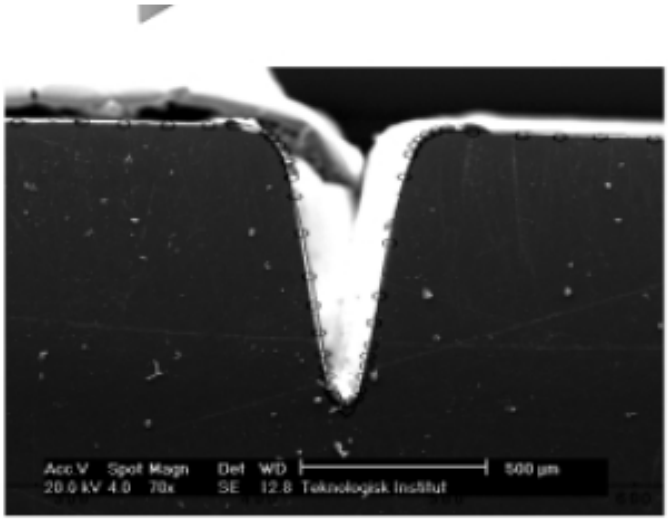

Figure 54: Cross section of PMMA created by a single beam pass of a CO_2 laser [35]

However, there are systems in literature that address these issues using a thermal annealing treatment, after the laser photoablation [32, 50]. While most papers make additional use of

surface modification to increase bonding strength, an approach that is beyond the scope of this project, it remains evident that solutions to this material drawback can be found in the literature.

Another technique, hot embossing, that would also have been appropriate for this project, uses a prefabricated mold, in combination with heat and pressure, to press the design into the PMMA. This approach often involves the use of a piece of equipment very similar to a tensile testing apparatus used in compression. However, the plates used to apply pressure are fitted to be heated and cooled quickly. This is due to PMMA having a glass transition temperature of approximately 106 C°, an elastic modulus of 3.1 Gigapascals, and a need to rapidly quench the material [51, 52]. The resolution of this approach is generally only limited by the resolution of the mold used to press the PMMA and would, therefore, be of considerably higher resolution than photoablation. However, the proper equipment did not exist at Cal Poly and would need to be purchased or built.

VI Bibliography

1. Chin, C.D., V. Linder, and S.K. Sia, *Lab-on-a-chip devices for global health: Past studies and future opportunities.* Lab on a Chip, 2007. **7**(1): p. 41-41.
2. Price, C.P., A.S. John, and J.M. Hicks, *Point-of-care testing*2004: Amer. Assoc. for Clinical Chemistry.
3. Lichtenberg, J., *Sample pretreatment on microfabricated devices.* Talanta, 2002. **56**(2): p. 233-266.
4. Pawliszyn, J., *Sampling and sample preparation for field and laboratory : fundamentals and new directions in sample preparation*. 1st ed. Comprehensive analytical chemistry2002, Amsterdam ; Boston: Elsevier Science. xxxiv, 1131 p.
5. Mohapatra, S.N., K.L. Costeloe, and D.W. Hill, *Blood resistivity and its implications for the calculation of cardiac output by the thoracic electrical impedance technique.* Intensive Care Med, 1977. **3**(2): p. 63-7.
6. Trutman, E.D. and R.S. Newbower, *A Practical Analysis of the Electrical Conductivity of Blood.* Biomedical Engineering, IEEE Transactions on, 1983. **BME-30**(3): p. 141-154.
7. Gabriel, C., A. Peyman, and E.H. Grant, *Electrical conductivity of tissue at frequencies below 1 MHz.* Phys Med Biol, 2009. **54**(16): p. 4863-78.
8. Baumann, S.B., et al., *The electrical conductivity of human cerebrospinal fluid at body temperature.* IEEE Trans Biomed Eng, 1997. **44**(3): p. 220-3.
9. Pawliszyn, J., *Solid phase microextraction : theory and practice*1997, New York: Wiley-VCH. xi, 247 p.
10. Abrams, T.J., *A PDMS SAMPLE PRETREATMENT DEVICE FOR THE OPTIMIZATION OF ELECTROKINETIC MANIPULATIONS OF BLOOD SERUM*, in *Biomedical Engineering*2009, California State Polytechnic University: San Luis Obispo. p. 137.
11. Lichtenberg, J., N.F. de Rooij, and E. Verpoorte, *A microchip electrophoresis system with integrated in-plane electrodes for contactless conductivity detection.* ELECTROPHORESIS, 2002. **23**(21): p. 3769-80.
12. Stoeppler, M., *Sampling and sample preparation : practical guide for analytical chemists*1997, Berlin ; New York: Springer. xiv, 202 p.
13. de Mello, A.J. and N. Beard, *Dealing with real samples: sample pre-treatment in microfluidic systems.* Lab Chip, 2003. **3**(1): p. 11N-19N.
14. Mitra, S., *Sample preparation techniques in analytical chemistry*. Chemical analysis2003, Hoboken, N.J.: J. Wiley. xx, 458 p.
15. Verpoorte, E., *Microfluidic chips for clinical and forensic analysis.* ELECTROPHORESIS, 2002. **23**(5): p. 677-712.
16. Landers, J.P., *Handbook of capillary electrophoresis*1994, Boca Raton: CRC Press. 649 p.
17. Dolnik, V., *Capillary zone electrophoresis of serum proteins: study of separation variables.* J Chromatogr A, 1995. **709**(1): p. 99-110.
18. Camilleri, P., *Capillary electrophoresis : theory and practice*. 2nd ed. New directions in organic and biological chemistry1998, Boca Raton, Fla.: CRC Press. 552 p.
19. *Outbreak of Shigella flexneri and Shigella sonnei enterocolitis in men who have sex with men, Quebec, 1999 to 2001.* Canada communicable disease report = Releve des maladies transmissibles au Canada, 2005. **31**(8): p. 85-90.
20. Branca, F., et al., *Biomarkers in disease and health.* The British journal of nutrition, 2001. **86 Suppl 1**: p. S55-92.

21. Landers, J.P., *Handbook of capillary and microchip electrophoresis and associated microtechniques*. 3rd ed2008, Boca Raton: CRC Press. xxi, 1567 p., 6 p. of plates.
22. Universal Laser Systems, I., *X2-660 Laser Engraving and Cutting System Manual*, in *16008 North 81st Street*2005, Universal Laser Systems, Inc: Scottsdale, AZ.
23. Ready, J.F., *Industrial applications of lasers*. 2nd ed1997, San Diego: Academic Press. xxi, 599 p.
24. Klank, H., J.P. Kutter, and O. Geschke, *CO2-laser micromachining and back-end processing for rapid production of PMMA-based microfluidic systems.* Lab on a Chip, 2002. **2**(4): p. 242-246.
25. Bell, A.R. and et al., *Fast-electron transport in high-intensity short-pulse laser - solid experiments.* Plasma Physics and Controlled Fusion, 1997. **39**(5): p. 653.
26. Barbre, E.A., *LASER ETCHED PMMA MICROFLUIDIC CHIP DESIGN AND MANUFACTURE WITH APPLICATIONS IN CAPILLARY ZONE ELECTROPHORESIS*, in *Biomedical Engineering*2011, California State Polytechnic University: San Luis Obispo. p. 160.
27. SNAKENBORG, et al., *Microstructure fabrication with a CO[2] laser system*. Vol. 14. 2004, Bristol, ROYAUME-UNI: Institute of Physics. 8.
28. Galloway, M., et al., *Contact Conductivity Detection in Poly(methyl methacylate)-Based Microfluidic Devices for Analysis of Mono- and Polyanionic Molecules.* Analytical Chemistry, 2002. **74**(10): p. 2407-2415.
29. Liu, Y., D.O. Wipf, and C.S. Henry, *Conductivity detection for monitoring mixing reactions in microfluidic devices.* The Analyst, 2001. **126**(8): p. 1248-1251.
30. Moorthy, J., et al., *Microfluidic tectonics platform: A colorimetric, disposable botulinum toxin enzyme-linked immunosorbent assay system.* ELECTROPHORESIS, 2004. **25**(10-11): p. 1705-13.
31. P. Kim, K.W.K., M.C. Park, S.H. Lee, S.M. Kim and K.Y. Suh, *Soft lithography for microfluidics: a review.* Biochip J. , 2008. **2**(1): p. 1-11.
32. Cheng, J.-Y., et al., *Direct-write laser micromachining and universal surface modification of PMMA for device development.* Sensors and Actuators B: Chemical, 2004. **99**(1): p. 186-196.
33. Chen, Z., et al., *Vacuum-assisted thermal bonding of plastic capillary electrophoresis microchip imprinted with stainless steel template.* Journal of chromatography. A, 2004. **1038**(1-2): p. 239-45.
34. Sun, X., et al., *Rapid prototyping of poly(methyl methacrylate) microfluidic systems using solvent imprinting and bonding.* Journal of chromatography. A, 2007. **1162**(2): p. 162-6.
35. Jensen, M.F., et al., *Microstructure fabrication with a CO2 laser system: characterization and fabrication of cavities produced by raster scanning of the laser beam.* Lab Chip, 2003. **3**(4): p. 302-7.
36. Tsao, C.-W. and D.L. DeVoe, *Bonding of thermoplastic polymer microfluidics.* Microfluidics and Nanofluidics, 2008. **6**(1): p. 1-16.
37. Greer, J. and et al., *Comparison of glass etching to xurography prototyping of microfluidic channels for DNA melting analysis.* Journal of Micromechanics and Microengineering, 2007. **17**(12): p. 2407.
38. Reger, D.L., S.R. Goode, and D.W. Ball, *Chemistry: Principles and Practice*2009: Brooks/Cole.
39. Grafen, A. and R. Hails, *Modern statistics for the life sciences*2002: Oxford University Press.
40. Amor, Z., et al., *Fluoride removal from brackish water by electrodialysis.* Desalination, 2001. **133**(3): p. 215-223.

41. Nejedly, L. *Electrodialysis*. 2006; Available from: http://www.mega.cz/electrodialysis.html.
42. Ameridia, I. *The Electrodialysis Stack* Available from: http://www.ameridia.com/html/elep.html.
43. Qi, H., et al., *Fabrication and characterization of a polymethyl methacrylate continuous-flow PCR microfluidic chip using CO₂ laser ablation.* Microsystem Technologies, 2009. **15**(7): p. 1027-1030.
44. Probstein, R.F., *Physicochemical hydrodynamics : an introduction*. 2nd ed1994, New York: Wiley. xv, 400 p.
45. Kirby, B.J. and E.F. Hasselbrink, Jr., *Zeta potential of microfluidic substrates: 2. Data for polymers.* ELECTROPHORESIS, 2004. **25**(2): p. 203-13.
46. Nörtemann, K., J. Hilland, and U. Kaatze, *Dielectric Properties of Aqueous NaCl Solutions at Microwave Frequencies.* The Journal of Physical Chemistry A, 1997. **101**(37): p. 6864-6869.
47. Zhang and Han, *Viscosity and Density of Water + Sodium Chloride + Potassium Chloride Solutions at 298.15 K.* Journal of Chemical & Engineering Data, 1996. **41**(3): p. 516-520.
48. Christen, J.B. and A.G. Andreou, *Design, Fabrication, and Testing of a Hybrid CMOS/PDMS Microsystem for Cell Culture and Incubation.* Biomedical Circuits and Systems, IEEE Transactions on, 2007. **1**(1): p. 3-18.
49. Becker, H. and C. Gartner, *Polymer microfabrication methods for microfluidic analytical applications.* ELECTROPHORESIS, 2000. **21**(1): p. 12-26.
50. Zhu, X., et al., *Study of PMMA thermal bonding.* Microsystem Technologies, 2007. **13**(3): p. 403-407.
51. Becker, H. and U. Heim, *Hot embossing as a method for the fabrication of polymer high aspect ratio structures.* Sensors and Actuators A: Physical, 2000. **83**(1-3): p. 130-135.
52. Qi, S., et al., *Microfluidic devices fabricated in poly(methyl methacrylate) using hot-embossing with integrated sampling capillary and fiber optics for fluorescence detection.* Lab on a Chip, 2002. **2**(2): p. 88-95.